

AD-A092 628 UNIVERSITY COLL LONDON (ENGLAND) DEPT OF PHYSICS AND--ETC F/8 4/1
TROPOSPHERIC - STRATOSPHERIC TIDAL INVESTIGATIONS, DIURNAL AND --ETC(U)
DEC 77 G V GROVES AFOSR-77-3224

UNIVERSITY COLL LONDON (ENGLAND) DEPT OF PHYSICS AND--ETC F/6 4/1
TROPOSPHERIC - STRATOSPHERIC TIDAL INVESTIGATIONS. DIURNAL AND --ETC(U)
DEC 77 G V GROVES AFOSR-77-3224

AFGL-TR-80-0348

NL

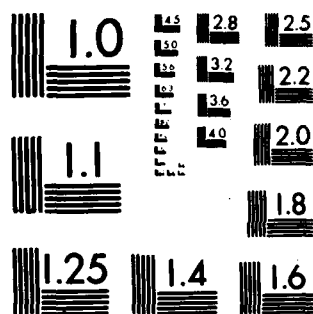
$$\frac{1}{2} \left(\frac{1}{2} + \frac{1}{2} \right) = \frac{1}{2}$$

DATE _____

100

1-8

DTIC



MICROCOPY RESOLUTION TEST CHART
NATIONAL BUREAU OF STANDARDS-1963 A

AFGL-TR-80-0348

LEVEL II

①

AD A092628

Grant number: AFOSR -77-3224

TROPOSPHERIC - STRATOSPHERIC TIDAL INVESTIGATIONS

Diurnal and semidiurnal wind oscillations in the stratosphere

G. V. Groves
Department of Physics and Astronomy,
University College London,
Gower Street, London WC1E 6BT,
England.

31 December 1977

DTIC
ELECTE
DEC 08 1980
S E

Scientific Report No. 1

1 December 1976 - 31 October 1977

Approved for public release; distribution unlimited.

Prepared for:

Air Force Geophysics Laboratory,
L. G. Hanscom Field, Bedford, Massachusetts 01730, USA.

and

European Office of Aerospace Research and Development,
London, England.

80 12 03 007

DDC FILE 001

UNCLASSIFIED

SECURITY CLASSIFICATION OF THIS PAGE (When Data Entered)

REPORT DOCUMENTATION PAGE		READ INSTRUCTIONS BEFORE COMPLETING FORM
1. REPORT NUMBER AFGL-TR-80-0348	2. GOVT ACCESSION NO. AD-A092628	3. RECIPIENT'S CATALOG NUMBER
4. TITLE (and Subtitle) TROPOSPHERIC - STRATOSPHERIC TIDAL INVESTIGATIONS.	5. TYPE OF REPORT, PERIOD COVERED Scientific Report, No. 1 1 Dec 76 - 31 Oct 77	6. PERFORMING ORG REPORT NUMBER
7. AUTHOR(s) GERALD V. GROVES	8. CONTRACT OR GRANT NUMBER(s) AFOSR-77-3224	
9. PERFORMING ORGANIZATION NAME AND ADDRESS DEPARTMENT OF PHYSICS AND ASTRONOMY UNIVERSITY COLLEGE LONDON GOWER STREET, LONDON, WC1 6BT, ENGLAND	10. PROGRAM ELEMENT, PROJECT, TASK AREA & WORK UNIT NUMBERS 668705AJ	
11. CONTROLLING OFFICE NAME AND ADDRESS AIR FORCE GEOPHYSICS LABORATORY Hanscom AFB, Massachusetts 01731 Monitor/William K. Vickery/LKD	12. REPORT DATE 31 DEC 1977	13. NUMBER OF PAGES 54
14. MONITORING AGENCY NAME & ADDRESS (if different from Controlling Office) EUROPEAN OFFICE OF AEROSPACE RESEARCH AND DEVELOPMENT, BOX 14, FPO, NEW YORK 09510, USA	15. SECURITY CLASS (of this report) UNCLASSIFIED	16. DECLASSIFICATION/DOWNGRADING SCHEDULE 17/05
16. DISTRIBUTION STATEMENT (of this Report) THIS DOCUMENT HAS BEEN APPROVED FOR PUBLIC RELEASES AND SALE; ITS DISTRIBUTION IS UNLIMITED.		
17. DISTRIBUTION STATEMENT (of the abstract entered in Block 20, if different from Report)		
18. SUPPLEMENTARY NOTES		
19. KEY WORDS (Continue on reverse side if necessary and identify by block number) TROPOSPHERE, STRATOSPHERE, TIDAL OSCILLATIONS, WINDS		
20. ABSTRACT (Continue on reverse side if necessary and identify by block number) Amplitudes and phases of diurnal and semidiurnal wind oscillations derived from 21 series of meteorological rocket launchings in the years 1965-74 are presented and discussed for different latitude regions in terms of the properties of diurnal and semidiurnal Hough modes of solar tidal oscillation. The investigation attempts to identify the likely ranges of modes (m,s,n), m = 1,2 which are compatible with excitation by ozone and water vapour heating and the observational results. Significant contributions from non-migrating modes (s & m) and from		

DD FORM 1 JAN 73 1473A EDITION OF 1 NOV 65 IS OBSOLETE

UNCLASSIFIED

SECURITY CLASSIFICATION OF THIS PAGE (When Data Entered)

361070

JW

20

non-tidal variations are in evidence for particular latitude regions.
A summary is given of a number of tentative conclusions that are reached
on the basis of the available data.

Accession For	
NTIS GRA&I	<input checked="checked" type="checkbox"/>
DDC TAB	<input type="checkbox"/>
Unannounced	<input type="checkbox"/>
Justification	
By _____	
Distribution _____	
Availability Codes	
Dist.	Available/or special
A	

1473B

Diurnal and semidiurnal wind oscillations
in the stratosphere

G. V. Groves

Department of Physics and Astronomy,
University College London,
England.

Abstract

Amplitudes and phases of diurnal and semidiurnal wind oscillations derived from 21 series of meteorological rocket launchings in the years 1965-74 are presented and discussed for different latitude regions in terms of the properties of diurnal and semidiurnal Hough modes of solar tidal oscillation. The investigation attempts to identify the likely ranges of modes (m,s,n) , $m = 1,2$ which are compatible with excitation by ozone and water vapour heating and the observational results. Significant contributions from non-migrating modes $(s \neq m)$ and from non-tidal variations are in evidence for particular latitude regions. A summary is given of a number of tentative conclusions that are reached on the basis of the available data.

PERMANENT RECORD COPY
DO NOT REMOVE FROM FILE

CONTENTS

	page
Introduction	3
Method of harmonic analysis of data	6
Equivalent depths of solar diurnal modes (1,s,n)	7
Diurnal winds at Fort Churchill (58.7°N, 93.8°W)	10
Diurnal winds at mid latitudes	13
Diurnal winds at low latitudes	17
Equivalent depths of solar semidiurnal modes (2,s,n)	21
Semidiurnal winds at latitudes greater than 30°	22
Semidiurnal winds at latitudes less than 30°	25
Discussion and conclusions	27
Diurnal components	29
Semidiurnal components	31
Acknowledgements	33
References	34
Figure captions	36

1. Introduction

Wind oscillations observed in the stratosphere by rocket techniques have previously been compared with results calculated by classical tidal theory (Reed et al., 1969). More recently comparisons have been made where the observed oscillations have been derived from relatively small numbers of rocket launchings extending over just 1 to 3 days (Groves, 1976)

Care needs to be taken when interpreting oscillations derived from small samples of data obtained with perhaps only 8 to 10 launchings at a single site. The evaluation of significant diurnal and semidiurnal components may not necessarily reveal the true tidal oscillation if for example a non-stationary oscillation or one close to the tidal frequency were to predominate. Also the application of classical tidal theory to the real atmosphere is open to uncertainties with regard to the distribution of thermal excitation and the assumption that the unperturbed atmosphere is at rest.

In spite of the foregoing limitations, similar properties have been identified in observational and theoretical results notably in the phases of oscillations (i.e. the times of maximum value); the observed gradients of these with height being consistent with those of Hough modes (the eigensolutions of Laplace's tidal equation). Such gradients in stratospheric diurnal and semidiurnal phases vary between different dates and indicate a source of excitation at lower heights which may reasonably be associated with water vapour heating: the observed phase gradients are indeed consistent with those of Hough

modes whose vertical structure has close coupling with observed vertical distributions of tropospheric water vapour. These and other features of tidal theory and observation have been previously reviewed (Groves, 1976).

In the present paper the previous work is extended to include further sets of observational data and, on the theoretical side, solutions of Laplace's tidal equation for a wider range of mode parameters. A useful increase in the totality of observational results was achieved on 19-20 March 1974 when 70 rockets equipped with standard Datasonde instrumentation were launched at 8 western hemisphere sites by NASA Wallops Flight Center in cooperation with other agencies in order to study atmospheric tides and their latitudinal variation (Schmidlin et al., 1975). The locations of the 8 sites are shown in Fig.1. Simultaneous launchings have been held on one previous occasion, on 23-25 October 1968, at the four sites of Ascension Is., Cape Kennedy, Fort Churchill and Thule. Otherwise diurnal series of launchings have been conducted on different dates at various low, mid and high latitude sites. Rocket-sonde instrumentation has been employed throughout except for a series of 13 rocket-grenade launchings at Kourou on 19-22 September 1971 (Smith et. al., 1974) and an extended series of rocket-grenade launchings at Natal in 1966-68 (Smith et. al., 1968, 1969, 1970). Diurnal launch series for which results are presented in this paper are listed in Table 1. Except where specific references are given the source of data has been the Meteorology Data Reports of World Data Center A.

TABLE 1. Diurnal launch series 1965-74.

Site	lat.	long.W	date	no. of successful launchings
Thule	76°33'N	68°49'	24-26 Oct 1968	14
Fort Churchill	58°44'	93°49'	6-8 Sept 1966	10
			8-9 Sept 1966	10
			4-5 Jan 1968	12
			23-25 Oct 1968	18
			19-20 Mar 1974	8
Wallops Is.	37°50'	75°29'	19-20 Mar 1974	13
Arenosillo	37°06'	06°44'	24-28 Feb 1970	27
White Sands	32°23'	106°29'	30 Jun-2 Jul 1965	17
			9-11 Oct 1965	16
Cape Kennedy	28°27'	80°32'	13-15 Dec 1967	25*
			23-25 Oct 1968	17
Antigua	17°09'	61°47'	19-20 Mar 1974	8
Fort Sherman	09°20'	79°59'	19-20 Mar 1974	8
Kourou	05°08'	52°37'	19-22 Sept 1971	13
			19-20 Mar 1974	10
Natal	05°55'S	35°10'	1966-68	24
			19-20 Mar 1974	8
Ascension Is.	07°59'	14°25'	11-12 Apr 1966	13
			12-13 Apr 1966	13
			24-26 Oct 1968	14
			19-20 Mar 1974	8
Mar Chiquita	37°45'	57°25'	19-20 Mar 1974	7

* Also analysed as 13-14 Dec 1967 (12 launchings) and 14-15 Dec 1967 (14 launchings).

2. Method of harmonic analysis of data

Assuming that a meteorological parameter \mathcal{V} may be represented by mean, diurnal and semidiurnal components, we write

$$\mathcal{V} = \mathcal{V}_0 + A_1 \cos \frac{1}{12} \pi t + B_1 \sin \frac{1}{12} \pi t + A_2 \cos \frac{1}{6} \pi t + B_2 \sin \frac{1}{6} \pi t \quad (1)$$

where t is local mean time in hours, departures from apparent local solar time being neglected. \mathcal{V}_0 , A_1 , B_1 , A_2 , B_2 are five unknowns which may be determined together with estimates of their standard deviations by the method of least squares from a series of more than five observations. The analysis has been described previously (Groves 1967) and does not require equal time intervals between observations. The analysis permits different weights to be associated with a sequence of observed values, but in the absence of any indication to the contrary all values have been weighted equally. Results are presented below in terms of the amplitudes and phases of the harmonic components which may be readily calculated from the values determined for the A's and B's in (1) : phase is expressed by the local time at which an oscillation maximizes.

The horizontal lines in plots of observational results below are centred on the least-squares calculated value of a quantity and are equal in length to two standard deviations. At heights where amplitudes are small, phases become indeterminate as indicated by very large error bars or a data point in brackets. Large standard deviations may also arise if a significant variation additional to those expressed by (1) is present. Attention has therefore been given to the removal of a background trend by replacing \mathcal{V}_0 in (1) by a polynomial in time.

When the total observing time exceeded two days, a cubic has been adopted

$$v_o = v_{o0} + v_{o1}t + v_{o2}t^2 + v_{o3}t^3 \quad (2)$$

Many series of launchings extend over only one day and in most cases the analysis of these has been carried out with v_o expressed linearly in time : in other cases where there are no more than 8 launchings in a series, the analysis has been carried out with v_o independent of time.

3. Equivalent depths of solar diurnal modes (1,s,n)

Associated with the eigenvalues of Laplace's tidal equation are modes of oscillation which for solar excitation may be designated by $S_n^{m,s}$ or $(m,s,n)_S$. The latter notation is adopted here and abbreviated to (m,s,n) as solar excitation is understood. Oscillations at the fundamental and higher harmonic frequencies have $m = 1, 2, \dots$. The zonal wave number s is taken positive for a westward travelling mode and negative for an eastward travelling mode, $|s|$ being the number of wavelengths that fit a circle of latitude. (A possible alternative notation would be m negative for an eastward travelling wave and s non-negative.) The meridional wave number n is assigned according to a prescribed scheme of notation.

Modes for which $s = m$ travel westward at the same rate as the Sun and have the same dependence on solar local time at all longitudes. Mode designation may then be abbreviated to (m,n) . Such modes, which are referred to as migrating modes, would arise with insolational

heating and a distribution of absorbing constituent that is independent of longitude. Variations with longitude of, say, water vapour give rise to modes having $s \neq m$. It may be noted that modes with $s = m$ dominate those with $s \neq m$ in an analysis of global distributions of surface pressure data for solar diurnal and semidiurnal components (Haurwitz and Cowley, 1973). The amplitude of the diurnal ($m = 1$) oscillation of the $s = 1$ wave (i.e. the superposition of all $(1,1,n)$ modes) is about 4 times greater than that of any other wave ($s \neq 1$). For the semidiurnal ($m = 2$) barometric oscillation the $s = 2$ wave (i.e. the superposition of all $(2,2,n)$ modes) has about 10 times the amplitude of any other wave ($s \neq 2$) on account of stratospheric heating which generates a large response at the surface through the $(2,2,2)$ mode.

For solar diurnal modes, eigenvalues ξ of Laplace's tidal equation have been calculated from relations given by Longuet-Higgins (1968) and Chapman and Lindzen (1970). The corresponding equivalent depths were then obtained as

$$h = 4a^2\omega^2 / g\xi \quad (3)$$

where a , g and ω are values of the Earth's radius, gravitational acceleration and sidereal angular velocity respectively ($4a^2\omega^2/g = 88.1$ km). In Fig.2 values of h are plotted for s in the range -12 to 14 and different n assigned as far as possible according to the notation employed by Chapman and Lindzen (1970). Two sequences of modes then remain with n unassigned. One of these exists only for $s \leq 0$ and has been given $n = 0$. The other is the sequence of eastward travelling

modes on the left-hand side of Fig.2. These are the type 3 modes of Longuet-Higgins (1968) being asymptotically Kelvin waves of velocity $(gh)^{\frac{1}{2}}$ as $h \rightarrow 0$, i.e. as $\epsilon \rightarrow \infty$. For large ϵ ,

$$\frac{m}{2(-s)} \sim \frac{1}{\epsilon^{\frac{1}{2}}} + \frac{1}{4\epsilon} \quad (4)$$

where $m = 1$ (the difference between solar and sidereal rates of rotation being neglected). It is found that the values of ϵ from (3) corresponding to the accurately calculated values of h (Fig.2) approximate (4) very closely yielding m to within 1.5% of unity for $s = -1$ and even more closely for larger $-s$. The notation $(1, s, K)$ is introduced for this sequence of modes.

Equivalent depth h is a useful indicator of the vertical properties of a mode which in the absence of dissipation and within the framework of classical theory depend solely on h and atmospheric scale height H . For small positive h the vertical structure is oscillatory, the wavelength being $2\pi H(\kappa H/h - 0.25)^{-\frac{1}{2}}$ for an atmosphere of constant scale height, where $\kappa = (\gamma - 1)/\gamma$ and γ is the ratio of specific heats of air. For small negative h the vertical structure decays exponentially over a distance $H(0.25 - \kappa H/h)^{-\frac{1}{2}}$ away from a region of excitation. Typical values for these parameters of the vertical structure are indicated on the right-hand side of Fig.2. For a relatively small range of values of $h \approx 4\kappa H$, wavelengths and decay distances become large and the vertical structure may be described as dynamically coupled. Fig.2 shows that this range of h is remote from the equivalent depths of all migrating modes $(1, 1, n)$ and is approached by at most

three other modes, namely $(1,-1,K)$, $(1,-2,K)$ and $(1,0,0)$. Fig.2 also shows that the wavelengths and decay distances of a sequence of modes shorten as $|s-1|$ increases. Vertical wavelengths of migrating modes are nearly 30 km for $(1,1,1)$ and decrease as n increases; that of $(1,1,4)$ being approximately 10 km. Exponential decay distances are about $2H$ for $(1,1,-1)$ and decrease as $-n$ increases, becoming $0.5H$ for $n = -5$ and -6 . Modes with negative n are also referred to as trapped and those with positive n as propagating modes. The terms positive and negative modes will be used to signify modes having $n > 0$ and < 0 respectively.

The ranges of modes likely to be excited by water vapour heating and ozone heating respectively are indicated in Fig.2. If mode wavelength is shorter than or comparable with the mean depth of the heating, the effect of the heating as a source of tidal excitation is reduced by self-cancellation as previously described (Groves, 1975a, 1976). Ozone heating, on account of its greater depth, is therefore incapable of exciting the shorter wavelength modes (indicated by the double vertical line) which are very effectively excited by water vapour heating.

4. Diurnal winds at Fort Churchill (58.7°N , 93.8°W)

Properties of the vertical structure of positive and negative modes are relevant to the interpretation of stratospheric oscillations at different latitudes. Fig.2 shows that negative-mode decay distances are $\leq H$ and hence, as H is about 7 km, the atmospheric response to tropospheric negative-mode excitations (notably by water vapour heating) is confined to the lower atmosphere. Likewise the response to negative-mode excitations by ozone heating is confined to the stratosphere and lower mesosphere. In contrast, amplitudes of positive modes increase with

height (until dissipation becomes important), and tropospheric excitations are capable of producing a significant oscillation at stratospheric heights. However the Hough functions \textcircled{P} for positive modes (Fig.3) are confined to low and mid latitudes, and hence at high latitudes stratospheric oscillations should consist predominantly of superimposed negative modes (Fig.4). In particular, if ozone heating is independent of longitude such (trapped) modes would travel westward with the Sun and have the same dependence on local time at all longitudes and heights. The height independence of phase at high latitude was confirmed by the analysis of Reed et al. (1969) of summer data between 30 and 60 km from the combined stations of Fort Churchill and Fort Greely (64.0°N , 145.7°W) for the diurnal S-N wind oscillation. Observed values of S-N wind phase were very close to 12 noon, the value which accords theoretically with an expected 12 noon phase for the heating rate.

Fig.5 shows S-N and W-E diurnal winds for Fort Churchill obtained from series of launchings conducted on the dates stated. The results are independent of those of Reed et al. (1969) which were derived from data widely distributed in time over the summer months of several years prior to and including 1966. The number of launchings in each series is shown in Table 1, although data from all launchings may not be available at every height. S-N wind phases are close to 12 noon with the notable exceptions to be discussed below of 4-5 January 1968 and certain heights below 45 km. For the W-E wind oscillation the corresponding phase should be 1800 hr as rotation of the wind vector is theoretically clockwise. With the same exceptions this value is

fairly well supported observationally. The two launch series in September 1966 comprise the first 10 and last 10 launchings respectively of a series of 19 launchings at 4 hr intervals over 3 days.

Below 40 km ozone lifetimes increase sufficiently for atmospheric motion to become an effective transport mechanism and longitudinal asymmetries in ozone distribution arise (Heath et al., 1973; Krueger et al., 1973; Dütsch, 1974). The maximum heating rate could then be at a longitude other than the subsolar longitude and phases of the atmospheric wind or temperature response would not generally be the same at all longitudes when expressed in local time. The unusual phase profiles of 4-5 January 1968 also direct attention to the possibility of a disturbed ozone distribution, in this case up to 55 km, which for the time of year might arise from a stratospheric warming and its effect on temperature-dependent photochemistry (Barnett, et al., 1975). In December 1967 a major warming occurred which persisted into the beginning of 1968. By the end of December, the temperature gradient between polar and mid latitudes had reversed throughout the entire middle and upper stratosphere making the event the earliest major stratospheric warming ever recorded (ESSA, 1970; NOAA, 1971).

The amplitudes of S-N and W-E winds in Fig.5 generally increase with height reaching about 10 m/s at 50-60 km. The leading symmetric negative mode (1,1,-2) would be expected to contribute prominently to these oscillations and for this mode the S-N and W-E components are theoretically of comparable magnitude at the latitude of Fort Churchill: wind functions for negative modes are shown in Figs.6 and 7

from which it is seen that the (1,1,-2) W-E amplitude is 72% of the S-N amplitude at 59° latitude. For the (1,1,-1) mode the (W-E)/(S-N) amplitude ratio is similar (86%) but for the (1,1,-3) and (1,1,-4) modes W-E amplitudes are nearly 3 times S-N amplitudes. The general similarity of the observed S-N and W-E amplitude profiles (Fig.5) is therefore in accord with the theoretical properties of the leading symmetric and asymmetric trapped modes and differences of detail may be attributed to contributions from modes of higher order in n.

The W-E wind functions Θ_U (Figs.6 and 8) and the S-N wind functions Θ_V (Figs.7 and 9) are related to the corresponding Hough functions Θ (Figs.3 and 4) by

$$\Theta_U = \frac{1}{f^2 - \cos^2 \theta} \left(\frac{\cos \theta}{f} \frac{d}{d\theta} + \frac{\sin \theta}{f} \right) \Theta \quad (5)$$

$$\Theta_V = \frac{1}{f^2 - \cos^2 \theta} \left(\frac{d}{d\theta} + \frac{\sin \theta \cot \theta}{f} \right) \Theta \quad (6)$$

where

$$f = \sigma / 2\omega \quad (7)$$

θ being colatitude and σ the angular frequency of the oscillation, i.e. the solar diurnal angular velocity.

5. Diurnal winds at mid latitudes

Wind functions for positive modes (Figs.8 and 9) show that the contributions from these modes increase rapidly between about 40° and 25° latitude reaching a maximum in the vicinity of 20° in contrast to negative-mode contributions which decrease equatorwards of 40° (Figs.6 and 7). Consequently on moving from Fort Churchill to

mid latitudes tropospheric positive-mode excitations can be expected to contribute increasingly to stratospheric diurnal oscillations. Observationally, a change from predominantly negative modes at high latitude to predominantly positive modes at low latitude was well supported by the analysis of stratospheric S-N wind oscillations by Reed et al. (1969).

A notable feature of the W-E and S-N wind functions for positive modes is their approximate equality for given s and n (to within about 20%) at latitudes between about 20° and 40° for many of the modes plotted in Figs.8 and 9. An examination of numerical values shows that the approximate equality holds well for $s \geq 0$ over this range of latitudes, but for $s < 0$ the latitude range depends on n and narrows as $-s$ increases. (Thus if $s = -2$ approximate equality (to within about 20%) holds for $n = 1$ from only 19° to 27° and for $n = 3$ from 23° to 33° ; if $s = -4$, it holds for $n = 1$ from only 16° to 21° and for $n = 3$ from 22° to 29° ; and if $s = -6$ it holds for $n = 1$ from only 14° to 17° , and for $n = 3$ from 20° to 26° latitude). Hence, provided certain modes of negative s are not of relatively large amplitude, approximately equal W-E and S-N wind profiles should be observed at latitudes between about 20° and 40° for whatever combination of other modes may be present. Also from the signs of the W-E and S-N wind functions at these latitudes (Figs.8 and 9) and the relevant equations of tidal theory, it follows that the rotation of the diurnal wind vector should be clockwise in the northern hemisphere and anticlockwise in the southern hemisphere for whatever combination of such modes

may be present.

The above theoretical properties are well supported by the observations at Cape Kennedy (28.4°N , 80.5°W) on 24-26 October 1968 (Fig.10), W-E and S-N amplitudes showing no significant differences and W-E phases being later than S-N phases by close to 6 hrs. The phase profiles are compared in Fig.10 with theoretical phases (the straight lines) for the (1,1,1) to (1,1,5) modes and indicate the presence of modes of a higher order in n and/or $|s|$ than the leading (1,1,1) mode. For a second series of Cape Kennedy launchings on 13-15 December 1967 (Fig.10), less than half the results are consistent with the above properties, W-E and S-N amplitudes showing conspicuous differences. In this case modes having negative s (for which the W-E and S-N wind functions differ at the latitude of Cape Kennedy) may be significant or a more general disturbance may be distorting or masking the tidal oscillation. Although the major stratospheric warming of December 1967 - January 1968 referred to above could be relevant, the slope of the phase profiles on 13-15 December 1967 points to a source of excitation that is located below 25 km and is therefore more likely to be tropospheric. These results will be further discussed in § 10 along with those for the semidiurnal component.

Data have also been analysed for diurnal winds at slightly higher latitudes than Cape Kennedy and the results (Figs.11 and 12) are generally consistent with the diurnal rotation of a wind vector of approximately constant amplitude at any given height. Reference lines at 12 hr and 18 hr have been added to the plots of S-N and W-E phases

respectively for the northern hemisphere sites to aid comparisons. The vertical profiles of S-N phase at White Sands (32.4°N , 106.5°W) are quite well reproduced with a 6 hr delay by the corresponding profiles of W-E phase. So also is that for Arenosillo (37.1°N , 6.7°W) where wind data were obtained at 75 to 95 km using a very light-weight chaff (Rose et al., 1972). For the southern hemisphere site of Mar Chiquita (37.7°S , 57.4°W), the observations are consistent with an anticlockwise rotation of the wind vector as theoretically predicted. Mar Chiquita phase profiles are approximately similar to those taken at the same time at Wallops Island (37.8°N , 75.5°W) which is at the same latitude (within 0.1°) in the opposite hemisphere. A 12 hr shift between S-N phases at the two sites indicates a tidal excitation that is predominantly symmetric with respect to the equator. Differences are however apparent between the Wallops Island and Mar Chiquita results particularly in amplitudes. Asymmetric modes could be expected to be responsible for minor differences between the two sites, but on analysis the differences are found to be too large to be reasonably accounted for in this way and a more likely origin for them is considered to be the 18.1° difference of longitude between the two sites and the presence of non-migrating modes ($s \neq 1$). For a longitude difference of this (relatively small) magnitude to produce any notable effect it would seem that at least some modes having $|s - 1| \geq 3$ would need to be reckoned with.

For the White Sands launchings of 30 June - 2 July 1965 a detailed report of the results has been given previously by Beyers, Miers and Reed (1966).

6. Diurnal winds at low latitudes

At latitudes of less than about 15° the S-N and W-E wind functions of positive modes become increasingly different in form. For n odd or $n = K$, S-N values change sign on crossing the equator whereas W-E values reach a maximum (or minimum) at the equator : for n even or zero, S-N values reach a maximum and W-E values change sign (Figs.8, 9, 13 and 14). At low latitude sites profiles of S-N and W-E phase and amplitude could therefore differ markedly; and the observational results in Figs.15 to 18 appear to confirm this expectation.

The results for Antigua (17.1°N , 61.8°W) show that W-E phases are again later than S-N phases by 6 hr at most heights except for the interval 36 to 51 km (Fig.15). It would appear that at the lower heights short wavelength modes are propagating in both components and that a change to longer wavelengths occurs in the W-E at 36 km and correspondingly in the S-N component in the region of 51 km.

Four sets of results for Ascension Island (8.0°S , 4.4°W) are compared in Fig.16. The two sets showing greatest similarity are the two for April 1966 which are based on the first 13 and last 13 launchings of a series of 24 over a 2-day period. A detailed analysis of the April 1966 data has been given by Beyers and Miers (1968) who noted considerable variation in both S-N and W-E components between the two days and concluded that the diurnal variation may have been masked or distorted by some other short-term disturbance. On closely comparing the two sets of April 1966 results in Fig.16, it is found that about 40% of both S-N and W-E phases on the second

day are significantly different from those on the first day: the results appear to represent oscillations of both tidal and non-tidal origin. For other low-latitude oscillations reported here no ready indication is generally available of the extent to which their origin is tidal or not as launch series are too short to compare consecutive cycles. Although in the following discussion the observed oscillations are referred to as tidal it is possible that for some of them this may not be the case.

For the three Ascension Island launch dates the phase and amplitude profiles obtained are different except over certain short isolated intervals of height. It may however be noted that the phase profiles have a general similarity with those at Cape Kennedy with respect to their gradients with height which correspond to modes of higher order in n and/or $|s|$ than the leading (1,1,1) mode. It may also be noted that S-N and W-E amplitudes lie within similar ranges of magnitude. If only migrating modes ($s = 1$) were propagating, the wind functions for Ascension Island (Figs.8 and 9) would have S-N values noticeably in excess of W-E values (by a factor of 2.1 for $n = 1$ and by larger factors for $n > 1$). However for many other modes ($s \neq 1$) W-E wind functions change with s such that at low latitude they become comparable with S-N values which change relatively slowly with s (Figs.8 and 9). Hence a significant low latitude contribution from non-migrating modes (with perhaps $|s| \geq 6$) may be inferred on the basis of S-N and W-E components being of comparable amplitude.

Modes of the sequences $n = 0$ and $n = K$ become likely contributors to atmospheric oscillations if a fairly high order of longitudinal variation is present in the source of excitation: their wind functions (Figs.13 and 14) attain increasingly large values as $-s$ increases, and for $-s = 8$ to 14 approximately their vertical structure is highly compatible with excitation by water vapour heating (Fig.2). The $n = 0$ sequence of modes have equatorially asymmetric Hough functions and S-N and W-E wind functions of similar magnitude: for the $n = K$ sequence, Hough functions are symmetric and the wind oscillation is almost entirely in the W-E direction with equatorial symmetry.

A comparison between the results for Fort Sherman (9.3°N , 80.0°W) in Fig.17 and those taken on the same date (19-20 March 1974) at Ascension Island is of interest as the two sites are at nearly the same latitude in opposite hemispheres. A similar comparison in § 5 for Wallops Island and Mar Chiquita indicated a predominantly symmetric excitation with respect to the equator, but from Figs.16 and 17 the Fort Sherman and Ascension Island oscillations are seen to differ in phase and amplitude. These differences are attributed to the longitude dependency of non-migrating modes, the likely presence of which has already been discussed, and possibly to asymmetric modes of high $|s|$, say > 10 , which could be significant at low latitudes but not at mid latitudes. The same interpretation would apply to the 19-20 March 1974 results (Fig.18) for Kourou (5.1°N , 52.6°W) and Natal (5.9°S , 35.2°W), which are also sites at approximately

equal latitudes in opposite hemispheres and show very different phases and amplitudes. As the difference of longitude between these two sites is only 17.4° (compared with 65.6° for Fort Sherman / Ascension Island) main contributions are expected from modes of $|s - 1| \geq 3$.

Also shown in Fig.18 are results obtained by the rocket-grenade method on different earlier dates at Natal (Groves, 1974) and Kourou (Groves, 1975). The Natal results would be expected to reveal a component of oscillation that is steady for much of the year being derived from launchings distributed over an interval of 22 months. In contrast to the 19-20 March 1974 results for Kourou and Natal, the Kourou rocket-grenade wind phases (Fig.18) agree closely with those for Natal of 1966-68 (except at the lowest heights). As reported previously however (Groves, 1975 b) the Kourou temperature oscillation showed significant differences from that for Natal, indicating some change in the source of excitation (water vapour heating) for which the atmospheric response at the latitude of these sites was of observational significance in temperature only. Further evidence of changes in the source of excitation between different observing dates is provided by the wind results at Natal and Kourou on 19-20 March 1974 (Fig.18) which show significant differences from the corresponding rocket-grenade results. There are however similarities of phase at the respective sites over limited height regions (e.g. from 40 to 60 km in the Kourou S-N wind), which

taken with the rocket-grenade results signify that certain modes may be present for much of the time while others are of a shorter duration.

8. Equivalent depths of solar semidiurnal modes (2,s,n)

Corresponding to Fig.2 equivalent depths h are plotted in Fig.19 for solar semidiurnal modes (2,s,n) where s lies in the range -12 to 14 and n is assigned according to the usual notation (Chapman and Lindzen, 1970). As with diurnal modes there are two sequences with n unassigned. One exists only for $s \leq 0$ and is denoted by $n = 1$. The other for which equation (4) holds with $m = 2$ is denoted by $n = K$.

Fig.19 shows that no sequences of trapped modes exist comparable with negative diurnal modes, but that several modes fall in the categories of weakly trapped modes or of modes whose vertical structure is dynamically coupled. The leading migrating mode (2,2,2) has a vertical structure that is dynamically coupled, one consequence being the excitation by stratospheric ozone heating of a major part of the semidiurnal surface pressure oscillation. The vertical lines in Fig.19 which relate to ozone and water vapour heating are repeated from Fig.2. For a typical depth of water vapour heating of 8 km, excitation of semidiurnal modes is effective for sequences up to $n \approx 30$ whereas for diurnal modes sequences up to $n = 5$ are excited. The short horizontal lines in Fig.19 give h for $s = 1$ and the intermediate sequences.

9. Semidiurnal winds at latitudes greater than 30°

At high and mid latitudes a semidiurnal tidal wind vector rotates clockwise at northern latitudes and anticlockwise at southern latitudes its amplitude remaining approximately constant at any given height (Groves, 1976). This result, which follows from classical tidal theory and the approximate equality of S-N and W-E wind functions at high and mid latitudes, holds for non-migrating modes (both eastward and westward travelling) as well as for migrating modes (in terms of which it was previously stated) as may be seen from Figs.20 and 21. At high latitudes the S-N and W-E wind functions are practically equal, but as latitude decreases the range of W-E values becomes smaller than that of S-N values so that at 30° latitude they may differ by a factor of 2. Observed semidiurnal oscillations for high and mid latitudes have previously been found to support the above theoretical result (Groves, 1976). Further observations have now been analysed and will be presented in this section and the next.

Fig.22 shows semidiurnal wind phases and amplitudes at six different sites, data being available at Fort Churchill for four different dates. The 19 launchings of 6-9 September 1966 at Fort Churchill have been divided into two groups consisting of the first 10 and the last 10 launchings respectively, each group extending over three semidiurnal cycles: Fig.22 shows that the results of the first group are quite well reproduced by the second group. The various sets of data in Fig.22 are for latitudes greater than 30°

and support the theoretical results above, W-E phase being consistent with S-N phase increased by 3 hr (or decreased by 3 hr for the southern hemisphere site of Mar Chiquita). Such agreement is taken as evidence that a tidal oscillation is being resolved by these short series of observations.

For the latitude of Thule (76.5°N , 68.6°W), Figs.20 and 21 show that tidal wind oscillations arise only with modes for which $|s - 1|$ is small, i.e. 0,1 or possibly 2. The sloping phase profiles of the Thule results correspond to a vertical wavelength of about 15 km, which implies by Fig.19 the presence of modes having $n \approx 14$.

Fig.23 shows semidiurnal Hough functions for $n = 2, 7, 12, 17$ and s between -12 and 14, these being the latitudinal profiles of heating for the respective modes. Although a wide range of values of n and s would generally be required for a complete representation of the global distribution of heating, only those modes whose vertical structure corresponds with the vertical profile of heating will be effectively excited in the atmospheric response (as indicated by the vertical lines in Fig.19). These modes are approximately defined by $n + |s| \lesssim 30$ and contain propagating modes approximately defined by $14 \lesssim n + |s| \lesssim 22$ for which the coupling with water vapour heating is closest (as indicated by the double vertical lines in Fig.19).

At Fort Churchill, phase profiles tend to show a region of changing phase at the lower heights leading into a region of constant phase at about 35 to 40 km. Shorter vertical wavelengths (of less than 10 km) are present at the lower heights implying modes with higher values

of $|s|$ and/or n than discussed above for Thule. The wind functions (Figs.20 and 21) show that modes with higher $|s|$ (assuming that such excitations were present) could generate oscillations at Fort Churchill. For wavelengths of less than 10 km, Fig.19 indicates $n > 20$.

For ozone heating, under conditions of photochemical equilibrium, longitudinal independence can be expected with the (2,2,2) mode providing the main oscillation. The regions of constant phase that appear in parts of the Fort Churchill profiles may be indicating the predominance of this mode at these heights. Fig.19 shows other modes whose vertical structure is dynamically coupled, e.g. (2,s,2) where $|s - 1|$ is small (≤ 3). These may be excited by longitudinal variations in ozone heating (either below 40 km or at greater heights at the time of a stratospheric warming) and would also produce an atmospheric response of nearly constant phase with height. Due to the absence of trapped semidiurnal modes corresponding to diurnal negative modes, there can be no semidiurnal atmospheric response localized in the height region of ozone heating.

The Wallops Island and Mar Chiquita results (Fig.22) have previously been compared and discussed (Groves, 1976). Phase profiles are similar at both sites and a mainly equatorially symmetric excitation is indicated by the difference of about 6 hr between the S-N phases. The Mar Chiquita results provide confirmation of an anticlockwise rotation of the wind vector in the southern hemisphere. The slopes of the phase profiles indicate values for n of possibly 14 to 18. As with the diurnal component, recognizable differences between the

results for the two sites exist and are attributed to their 18.1° difference of longitude and the presence of non-migrating waves having, in this case, $|s - 2| \gg 3$.

The Arenosillo results are consistent with a clockwise rotation of the wind vector at the centre of the height range of observation, i.e. from about 82 to 88 km ; and it is at these heights where the chaff measuring technique is most effective.

The two sets of White Sands results show a clockwise rotating wind vector at about 70% of the observation heights. For a latitude of 32° , such agreement would seem to be quite reasonable.

10. Semidiurnal winds at latitudes less than 30°

The two sets of results for Cape Kennedy at 28.5° latitude are also consistent with a clockwise rotating wind vector at most observation heights (Fig.24) and could be grouped with the results in Fig.22. At lower latitudes W-E and S-N wind functions (Figs.20 and 21) become increasingly dissimilar and corresponding dissimilarities are to be expected between observed W-E and S-N wind oscillations. Observationally the results for Antigua, Fort Sherman and most other launch series in Fig.24 show conspicuous differences between W-E and S-N components which would appear to confirm this expectation.

The semidiurnal oscillations for Ascension Island on 11-12 and 12-13 April 1966 (Fig.24) change radically in both wind components between the two days, whereas only partial changes in the diurnal

component were noted in §6 (Fig.16). These results are in contrast to those of 6-9 September 1966 at Fort Churchill for which both diurnal (Fig.5) and semidiurnal profiles (Fig.22) were found to be quite similar between two consecutive intervals. It has also been possible to analyse the Cape Kennedy data of 13-15 December 1967 (Figs.10 and 22) as two consecutive groups and the results obtained are compared in Fig.25. For the diurnal oscillation, the S-N components are very similar whereas the W-E components are distinctly different. The non-tidal nature of the diurnal oscillation pointed out in §6, would therefore seem to be associated almost entirely with the W-E component. The semidiurnal oscillations for the two consecutive days (Fig.25) are similar to the results for the combined data (Fig.24) and would tend to confirm a tidal origin. As pointed out in §6, for other observed oscillations at low latitude there is generally no ready indication of the extent to which their origin is tidal or not. In the following discussion oscillations are assumed to be tidal although this might not always be the case. The April 1966 results at Ascension Island and the December 1967 results at Cape Kennedy show that either the diurnal or semidiurnal oscillation may be disturbed much more than the other.

The Ascension Island results of 24-26 October 1968 (Fig.24) are exceptional being consistent with an anticlockwise rotation of the wind vector at almost all heights. Such a result at a low latitude site is not without interpretation as a single tidal mode

would give either a clockwise or anticlockwise rotating wind vector whatever the latitude. It may be noted that a vertical wavelength of about 12 km is strongly in evidence in the phase profiles (Fig.24) and indicates the dominance in both S-N and W-E components of a single mode.

As with the diurnal component, semidiurnal S-N and W-E amplitudes at low latitudes (Fig.24) lie within comparable ranges of values and a difficulty arises in adequately accounting for W-E amplitudes unless, according to the wind functions (Figs.20, 21, 26 and 27), non-migrating modes ($s \neq 2$) of possibly $|s| \geq 6$ are main contributors. The differences between the 19-20 March 1974 results at the pairs of equatorially symmetrically located sites of Fort Sherman / Ascension Island and Kourou / Natal offer further general support for the presence of high-order non-migrating modes. The Hough functions and wind functions for $(2,s,1)$ and $(2,s,K)$ (Figs.26 and 27) are very similar to the corresponding diurnal functions (Figs.13 and 14) and are also likely contributors to atmospheric oscillations if a fairly high degree of longitudinal variation is present in the source of excitation (water vapour heating).

11. Discussion and conclusions

Diurnal and semidiurnal components of stratospheric wind variation derived from diurnal launch series (Table 1) have been presented and discussed in terms of the Hough modes of classical tidal theory.

Although for many launch series only 8 wind data values are available at any height it has nevertheless been possible to derive significant diurnal and

semidiurnal components of variation by the method of least-squares analysis. While such results are without doubt evidence of the variability of stratospheric winds, their immediate interpretation as tidal oscillations is only one of several possibilities. The traditional method of tidal discrimination is by analysis of long series of data and as only one or two cycles are available supporting evidence of an alternative nature has been sought.

At mid and high latitudes, W-E and S-N semidiurnal wind profiles should, according to classical tidal theory, be approximately equal apart from a 3hr phase shift corresponding to clockwise rotation in the N hemisphere or anticlockwise rotation in the S hemisphere. Observed W-E and S-N wind components are independent sets of data and hence comparisons between their derived semidiurnal components should test whether the tidal interpretation is at least tenable. Significant results from 13 series of launchings are available for mid and high latitudes (i.e. at Cape Kennedy and higher latitudes) and in all cases there is support for the above theoretical relationship. Conversely at low latitudes where the relationship would not generally be expected to hold, there is a convincing lack of observational support.

With some justification then an attempt has been made in this paper to interpret the stratospheric oscillations observed by diurnal launch series at different latitudes in terms of modes of tidal oscillation. An interpretation has been sought which is compatible not only with the observational results but also with ozone and

water vapour heating as sources of tidal excitation. Even so the distribution of available data limits the scope of the investigation to an identification of the ranges of mode parameters within which significant contributions are likely to be found. A number of tentative conclusions have been reached and are summarized below. No attempt is made to qualify the extent of the various identifications and associations proposed, but with due critical regard it is hoped that the summary will be helpful to further investigations. No account can be given of seasonal dependences as most of the available results were obtained at or close to an equinox.

(i) Diurnal components

At high latitudes stratospheric oscillations are superpositions of negative (trapped) modes $(1, s, n)$, $n \leq 0$ excited by ozone heating. Below about 40 km, longitudinal variations of ozone and consequent heating give rise to negative non-migrating ($s \neq 1$) modes in the same height range. Above about 45 km, negative migrating modes ($s = 1$) predominate except at the time of stratospheric warmings when longitudinal variations of ozone and consequent heating excite negative non-migrating modes in the height range of the stratospheric disturbance.

At mid latitudes the above (trapped) oscillations are supplemented by significant and sometimes dominant contributions of positive (propagating) modes excited by tropospheric heating. Excitation of positive modes by undisturbed ozone heating leads to an atmospheric response which is limited by self-cancellation to the $(1, 1, 1)$ mode.

This mode which is also excited by tropospheric heating is dominated in the stratosphere by modes of higher order in n and/or $|s|$ of tropospheric origin. Such higher-order modes, or at least some of them, are steady for only short intervals of time, possibly a few days, and would not be revealed unless data were collected with adequate frequency. Non-migrating positive modes contribute to mid-latitude oscillations with decreasing effect polewards of 30° latitude in accord with the diurnal wind functions. Such contributions are practically zero for $|s| \geq 6$, but are significant for smaller values including values such that $|s - 1| \geq 3$. The values of s that arise at mid-latitudes relate to the gross features of the global distribution of tropospheric heating: $s = 1$ relates to the longitudinal average of the distribution and other values of $|s|$ (up to about 6) relate to the main regions of high specific humidity such as Central America / Eastern Pacific, Africa and S. E. Asia. The contribution from eastward travelling modes ($s < 0$) is generally small compared with that of non-migrating westward travelling modes. The range of n extends from 1 to about 5 above which value mode vertical structure leads to self-cancellation of tropospheric heating as a tidal source.

At low latitudes trapped stratospheric modes make a minor contribution compared with that of propagating modes. In addition to the propagating modes of $|s| \leq 6$ which may be present at mid latitudes, it is possible for modes of higher $|s|$ to propagate at low latitudes given a suitable longitudinal variation in the low-latitude tropospheric heating. An upper limit is however set for $|s|$ by the increase of self-cancellation with

decrease of wavelength as $|s|$ increases, the limit being $|s| \approx 16$ and depending slightly on n . Temporal changes and spatial movements in the distribution of an atmospheric absorbing constituent could also prevent the establishment of steady (or quasi-steady) diurnal excitations for $|s|$ above a certain value according to the scale of distance over which such variations would average out. In consequence non-tidal contributions would effectively replace tidal contributions of higher $|s|$ appropriate to a non-varying atmosphere with radiational heating and could dominate the steady (or quasi-steady) tidal modes of lower $|s|$ that are still able to propagate in the real atmosphere. Upper limits for $|s|$ are not easily assessed but when regard is taken of the global distribution of water vapour and its variations it would seem at first sight that $|s|$ would be unlikely to attain the upper limit (≈ 16) set by self-cancellation and might at times be restricted to values ≤ 6 . As at mid latitudes, excitation of modes having $n \geq 5$ is ineffective due to self-cancellation of tropospheric heating as a tidal source : this leaves modes of the sequences $n = K$ and $n = 1, 3$ to represent most of the equatorial symmetry and modes of the sequences $n = 0, 2, 4$ to represent most of the asymmetry. Dissipation of wave energy is more rapid for modes of shorter wavelength and hence as height increases modes of higher n or $|s - 1|$ are attenuated relative to those of smaller n or $|s - 1|$.

(ii) Semidiurnal components

Both ozone heating and tropospheric heating are effective in exciting semidiurnal oscillations at stratospheric heights. Ozone heating excites modes which have nearly the same phase over a wide range of heights.

The (2,2,2) mode arises from the longitudinal average of the ozone distribution.

and longitudinal variations of ozone (whether below 40 km or at greater heights at the time of a stratospheric warming) give rise to non-migrating modes whose vertical structure is also dynamically coupled thereby introducing a longitudinal dependence into the (height independent) phase of the oscillation.

In the troposphere the excitation of modes $(2,s,n)$ is limited by self-cancellation to values of s and n such that $n + |s| \leq 30$. Significant contributions at stratospheric heights arise from propagating modes particularly those which are closely coupled with the vertical structure of the tropospheric source of excitation: for such a mode s and n satisfy $14 \leq n + |s| \leq 22$. When higher values of $|s|$ are present they are associated with lower values of n according to the above condition and propagate at latitudes equatorwards of about 40° : for very high $|s|$, say 12 to 20, the propagation would be confined to quite low latitudes. As with diurnal oscillations, non-tidal components may effectively replace the steady (or quasi-steady) tidal modes of higher $|s|$ appropriate to a non-varying atmosphere with radiational heating. Again the upper limits for $|s|$ are not readily assessed, but most values of $|s|$ up to about 6 would be expected to be present according to the gross features of the global distribution of tropospheric heating. As for diurnal components, dissipation of wave energy leads to the attenuation of modes of higher n or $|s| - 1$ relative to modes of longer wavelength as height increases.

Acknowledgements

The very able assistance of Miss A. M. Yeung with preparation and analysis of data and computer programming is gratefully acknowledged.

The detailed diagrams in this paper owe much to the efforts of Miss A. M. Yeung, Miss U. Campbell and members of the Departmental Photographic Group.

Sponsorship has been provided by the Air Force Geophysics Laboratory (AFGL), United States Air Force under Grant No. AFOSR-77-4224 and by the U.K. Meteorological Office.

References

- Barnett, J. J., J. T. Houghton, and J. A. Pyle, 1975 Quart. J. R. Met. Soc. 101, 245-257.
- Beyers, N. J. and B. T. Miers, 1968 J. atmos. Sci. 25, 155-159.
- Beyers, N. J., B. T. Miers, and K. J. Reed, 1966 J. atmos. Sci. 23, 325-336.
- Chapman, G. and R. S. Linzen, 1970 Atmospheric tides : thermal and gravitational, Dordrecht, Holland : R. Reidel Publishing Co.
- Hütsch, H. U. 1974 Can. J. Chem. 52, 1491-1504.
- EMSA 1970 Weekly Synoptic Analyses, 5-, 2-, and 0.4- Millibar Surfaces for 1967, EMSA Technical Report WB12.
- Groves, G. V. 1967 Space Research 7, 986-1000.
- Groves, G. V. 1974 J. Br. interplan. Soc. 27, 499-511.
- Groves, G. V. 1975a J. Br. interplan. Soc. 28, 797-809.
- Groves, G. V. 1975b J. Br. interplan. Soc. 28, 241-244.
- Groves, G. V. 1976 Proc. R. Soc. Lond. A. 351, 437-469.
- Haurwitz, B. and A. J. Cowley, 1975 Pure appl. Geophys. 121, 197-211.
- Heath, D. F., C. L. Mateer, and A. J. Krueger, 1975 Pure appl. Geophys. 121, 1247-1254.
- Krueger, A. J., D. F. Heath, and C. L. Mateer, 1975 Pure appl. Geophys. 121, 1255-1264.
- Longuet-Higgins, M. G. Phil. Trans. R. Soc. Lond. 1975 A, 262 511-607.
- NOAA 1971 Weekly Synoptic Analyses, 5-, 2-, and 0.4- Millibar Surfaces for 1968, NOAA Technical Report NWS 34.
- Reed, K. J., M. J. Card, and M. Siewinski, 1969 Mon. weath. rev. 97, 450-459.

Rose, G., H. U. Widdel, A. Azcárraga, and L. Sanchez, 1972 Phil.

Trans. R. Soc. Lond. A. 271, 509-528.

Schmidlin, F. J., Y. Yamasaki, A. Motta, and S. Brynsztein, 1975

NASA sp-3095, Washington, D.C.

Smith, W. S., J. S. Theon, J. F. Casey, and J. J. Horvath, 1970

NASA TR R-340, Washington, D.C.

Smith, W. S., J. S. Theon, P. C. Swartz, J. F. Casey, and J. J. Horvath

1969 NASA TR R-316, Washington, D.C.

Smith, W. S., J. S. Theon, P. C. Swartz, L. B. Katchen, and J. J. Horvath

1968 NASA TR R-288, Washington, D.C.

Smith, W. S., J. S. Theon, D. U. Wright, Jr., D. J. Ramsdale, and

J. J. Horvath, 1974 NASA TR R-416, Washington, D.C.

Figure captions

1. The eight sites from which diurnal series of rockets were launched on 19-20 March 1974.
2. Equivalent depths h of solar diurnal Hough modes $(1,s,n)$ for various s and n . A = modes whose Hough functions are equatorially asymmetric, S = modes whose Hough functions are equatorially symmetric. \equiv (double vertical lines) vertical structures of mode and heating correspond closely; --- (single vertical line) self-cancellation not significant; ---- (broken vertical line) self-cancellation significant; \downarrow limit where self-cancellation is practically complete.
3. Hough functions Θ for modes $(1,s,n)$, $n = 1, \dots, 4$.
4. Hough functions Θ for modes $(1,s,n)$, $n = -1, \dots, -4$.
5. Diurnal wind components at Fort Churchill.
6. W-E wind functions Θ_U for modes $(1,s,n)$, $n = -1, \dots, -4$.
7. S-N wind functions Θ_V for modes $(1,s,n)$, $n = -1, \dots, -4$.
8. W-E wind functions Θ_U for modes $(1,s,n)$, $n = 1, \dots, 4$.
9. S-N wind functions Θ_V for modes $(1,s,n)$, $n = 1, \dots, 4$.
10. Diurnal wind components at Cape Kennedy. The straight lines indicate the approximate theoretical slopes of the phase profiles of the first five positive migrating modes.
11. Diurnal wind components at White Sands, Wallops Island and Mar Chiquita.
12. Diurnal wind components at Arenosillo, 24-28 February 1970.
13. Hough functions Θ (upper row), S-N wind functions Θ_V (middle row) and W-E wind functions Θ_U (lower row) for modes $(1,s,K)$, $s = -1, -4, -8$, and -12 .

14. Hough functions Θ (upper row), S-N wind functions Θ_V (middle row) and W-E wind functions Θ_U (lower row) for modes $(1,s,C)$, $s = 0, -4, -8$ and -12 .
15. Diurnal wind components at Antigua, 19-20 March 1974.
16. Diurnal wind components at Ascension Island. (1) 11-12 April 1966; (2) 12-13 April 1966; (3) 24-26 October 1968; (4) 19-20 March 1974.
17. Diurnal wind components at Fort Sherman, 19-20 March 1974.
18. Diurnal wind components at Kourou and Natal. (1) Kourou, 19-22 September 1974; (2) Kourou, 19-20 March 1974; (3) Natal, 1966-68; (4) Natal, 19-20 March 1974.
19. Equivalent depths h of solar semidiurnal Hough modes $(2,s,n)$ for various s and n . (See caption to Fig. 2). The short horizontal lines give h for $s = 1$ and the intermediate values of n .
20. W-E wind functions Θ_U for modes $(2,s,n)$, $n = 2, 7, 12$ and 17 .
21. S-N wind functions Θ_V for modes $(2,s,n)$, $n = 2, 7, 12$ and 17 .
22. Semidiurnal wind components at latitudes greater than 30° .
 (1) Thule, 24-26 October 1968; (2) Fort Churchill, 4-5 September 1966; (3) Fort Churchill, 8-9 September 1966; (4) Fort Churchill, 4-5 January 1968; (5) Fort Churchill, 23-26 October 1968; (6) Fort Churchill, 19-20 March 1974; (7) Wallops Island, 19-20 March 1974; (8) Mar Chiquita, 19-20 March 1974; (9) Arenosillo, 24-28 February 1970; (10) White Sands, 30 June - 2 July 1965; (11) White Sands, 9-11 October 1964.
23. Hough functions Θ for modes $(2,s,n)$, $n = 2, 7, 12$ and 17 .

24. Semidiurnal wind components at latitudes less than 40° .
(1) Cape Kennedy, 13-15 December 1967; (2) Cape Kennedy, 23-25 October 1968; (3) Antigua, 19-20 March 1974; (4) Fort Sherman, 19-20 March 1974; (5) Kourou, 19-22 September 1971; (6) Kourou, 19-20 March 1974; (7) Natal, 19-20 March 1974; (8) Ascension Island, 11-12 April 1966; (9) Ascension Island, 12-13 April 1966; (10) Ascension Island, 24-26 October 1968; (11) Ascension Island, 19-20 March 1974.
25. Diurnal and semidiurnal wind components on two consecutive days at Cape Kennedy. (1) 13-14 December 1967; (2) 14-15 December 1967.
26. Hough functions Θ (upper row), S-N wind functions Θ_V (middle row) and W-E wind functions Θ_U (lower row) for modes (2,s,K), $s = -1, -4, -8$ and -12 .
27. Hough functions Θ (upper row), S-N wind functions Θ_V (middle row) and W-E wind functions Θ_U (lower row) for modes (2,s,1), $s = -1, -4, -8$ and -12 .

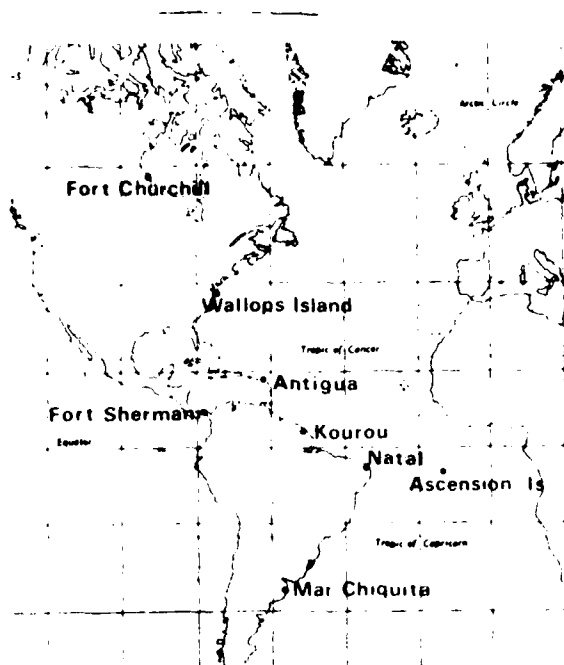


Fig.1. The eight sites from which diurnal series of rockets were launched on 19-20 March 1974.

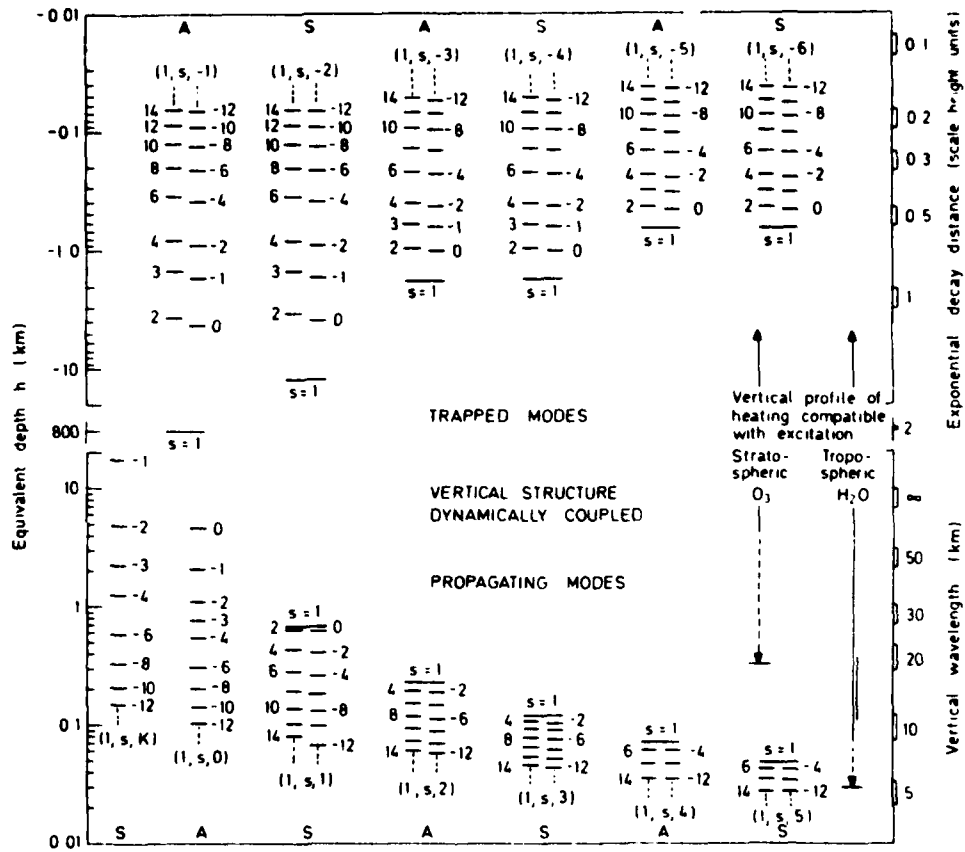


Fig.2. Equivalent depths h of solar diurnal Hough modes $(1, s, n)$ for various s and n . A = modes whose Hough functions are equatorially asymmetric, S = modes whose Hough functions are equatorially symmetric. \equiv (double vertical lines) vertical structures of mode and heating correspond closely; \equiv (single vertical line) self-cancellation not significant; \equiv (broken vertical line) self-cancellation significant; \downarrow limit where self-cancellation is practically complete.

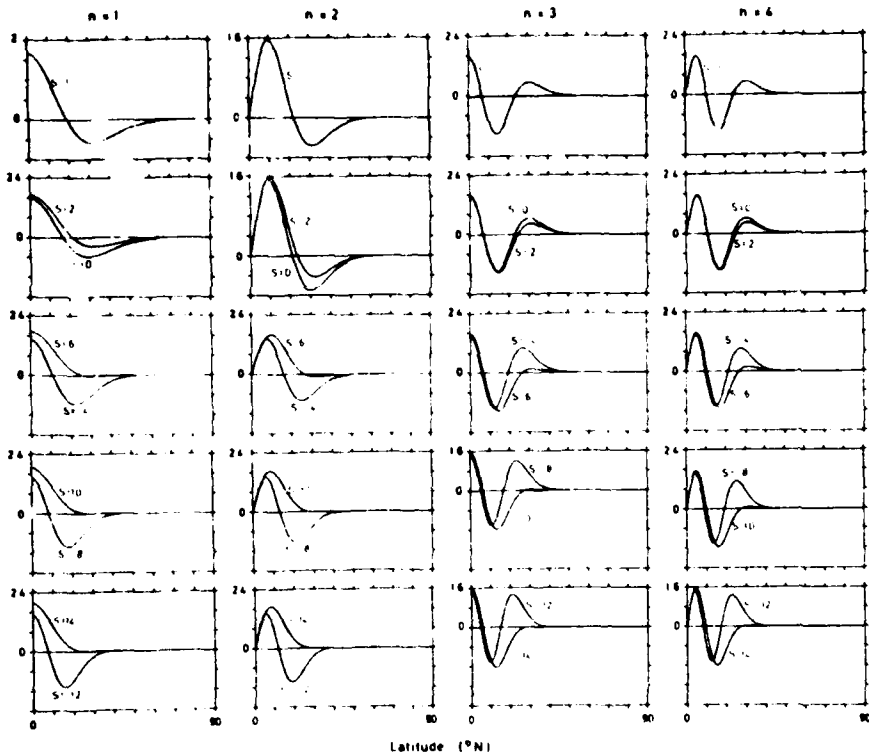


Fig.3. Hough functions Θ for modes $(1, s, n)$, $n = 1, \dots, 4$.

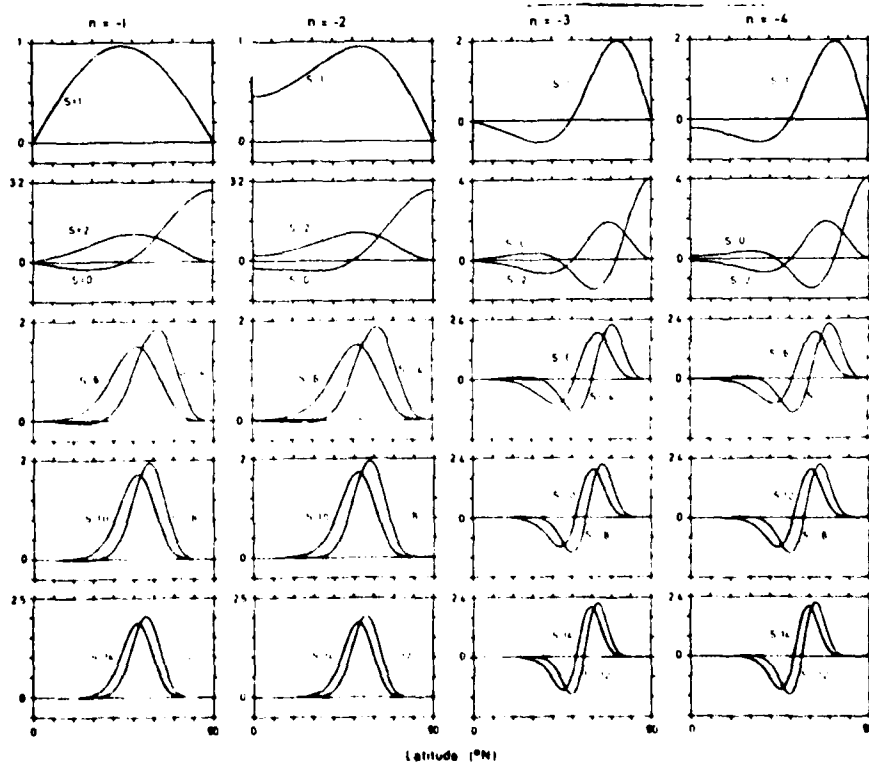


Fig. 1. Bound functions (a) for modes: (1,0,n), $n = -1, \dots, -4$.

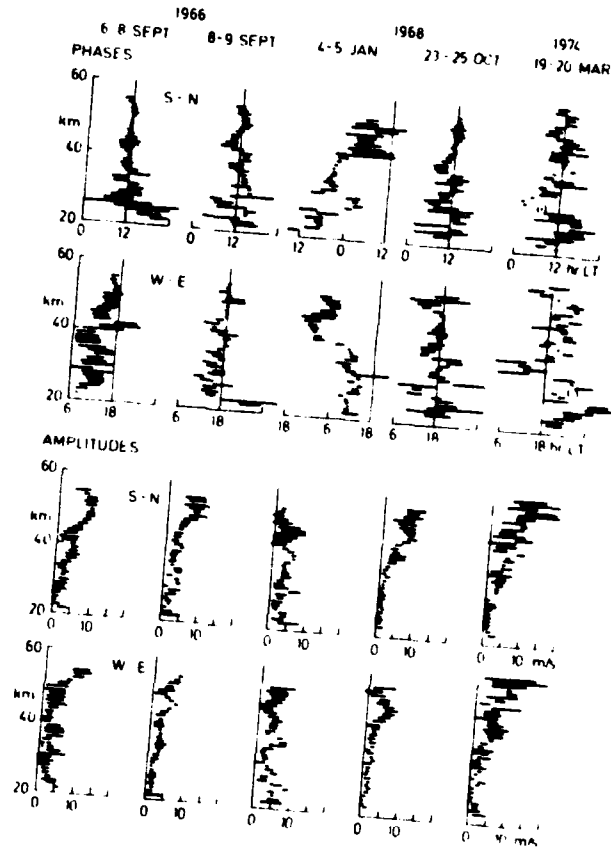


Fig.5. Diurnal wind components at Fort Churchill.

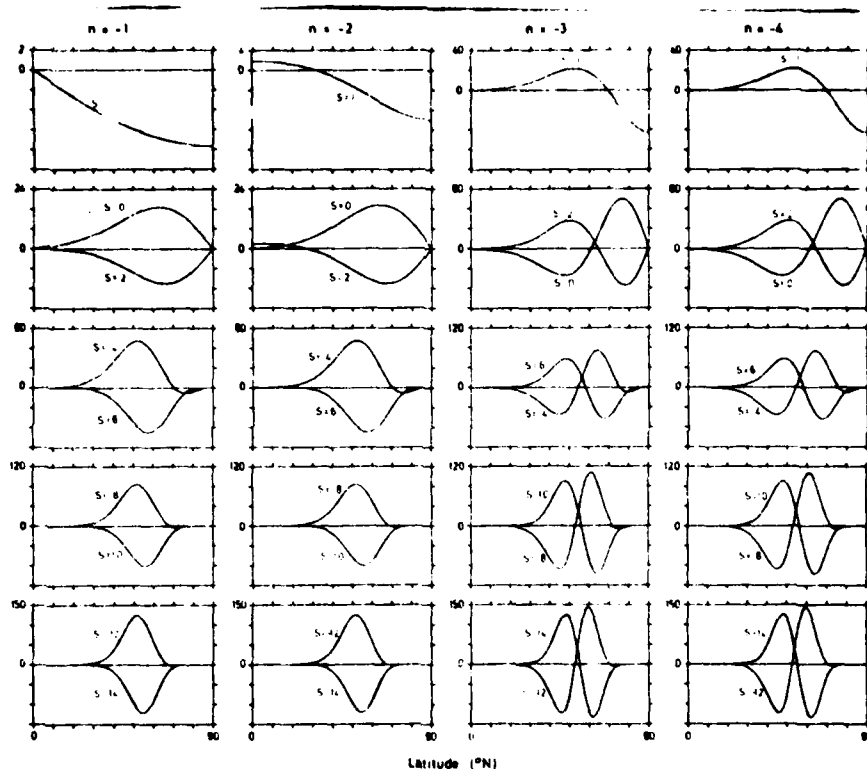


Fig.6. W-E wind functions Θ_U for modes $(1,s,n)$, $n = -1, \dots, -4$.

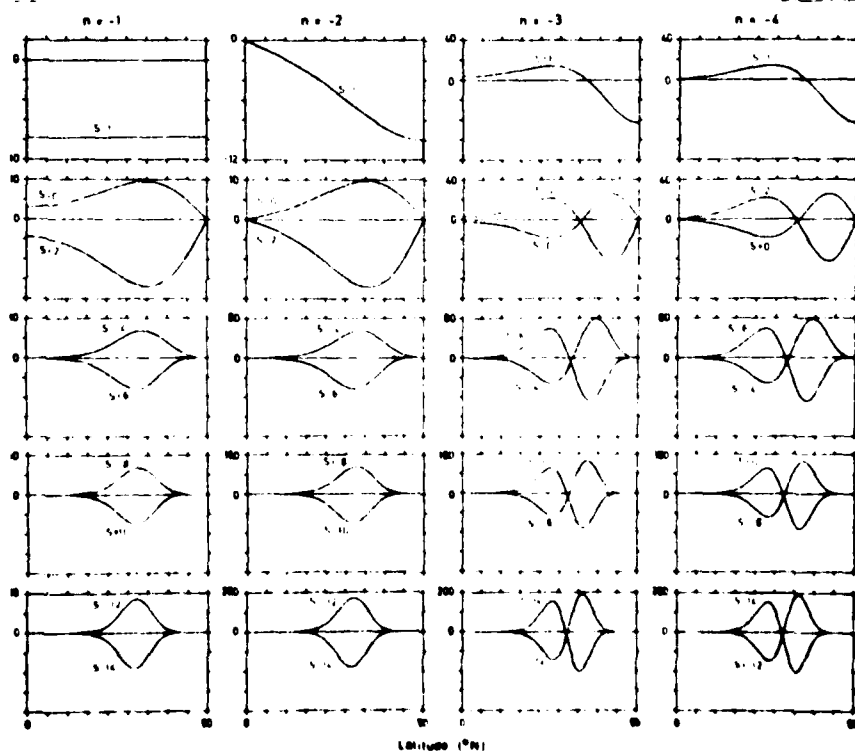


Fig.7. S-N wind functions Θ_V for modes $(1,s,n)$, $n = -1, \dots, -4$.

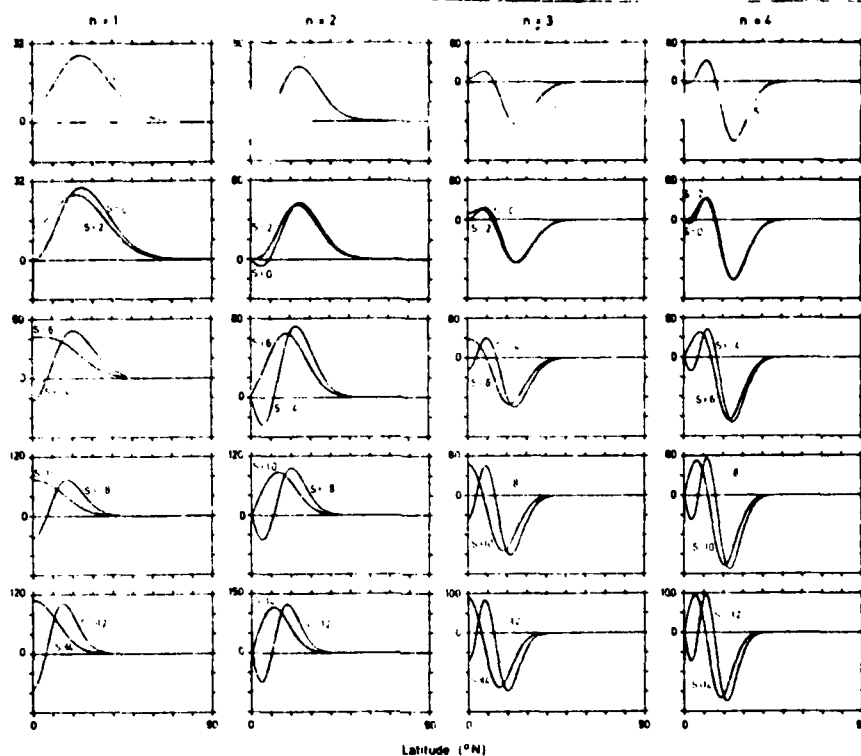


Fig. 8. w-E wind functions Θ_U for modes $(1, s, n)$, $n = 1, \dots, 4$.

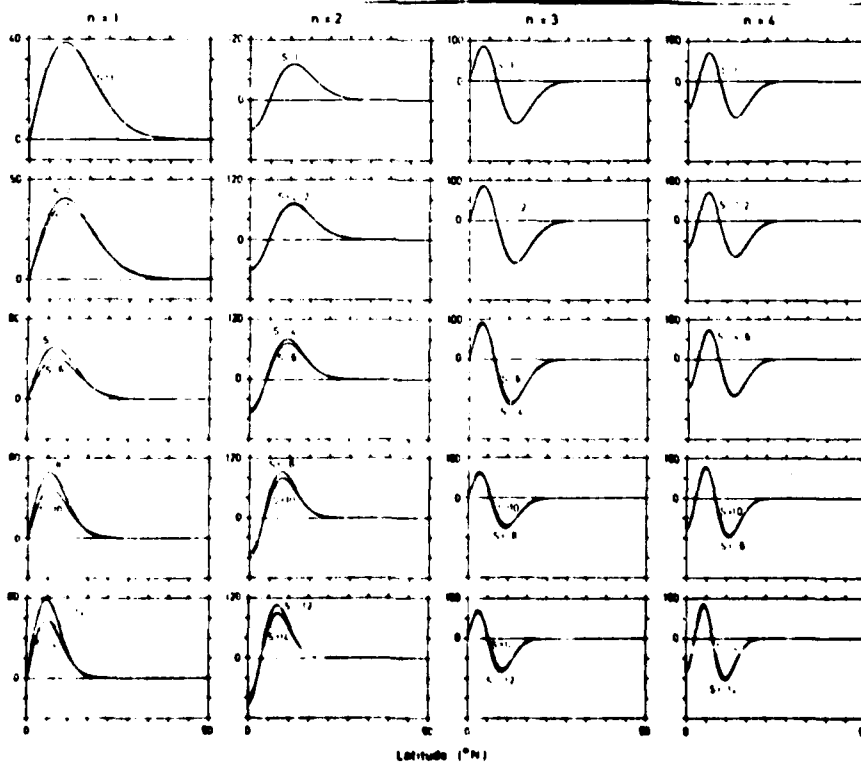


Fig. 9. S-N wind functions Θ_V for modes $(1, s, n)$, $n = 1, \dots, 4$.

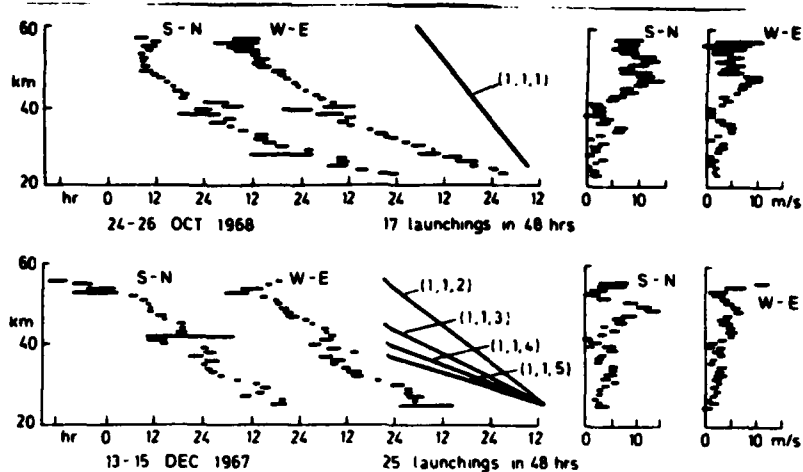


Fig.10. Diurnal wind components at Cape Kennedy. The straight lines indicate the approximate theoretical slopes of the phase profiles of the first five positive migrating modes.

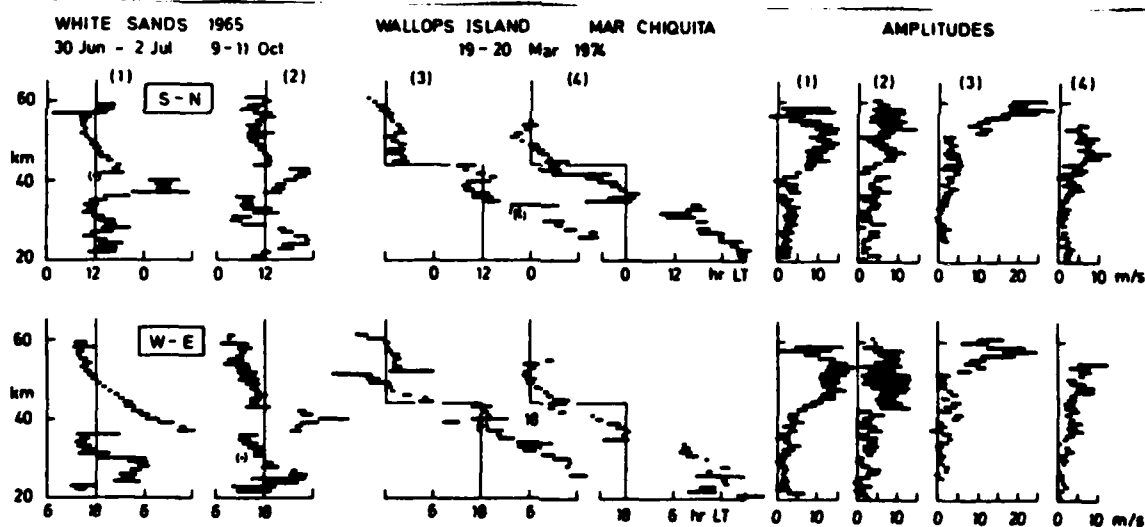


Fig.11. Diurnal wind components at White Sands, Wallops Island and Mar Chiquita.

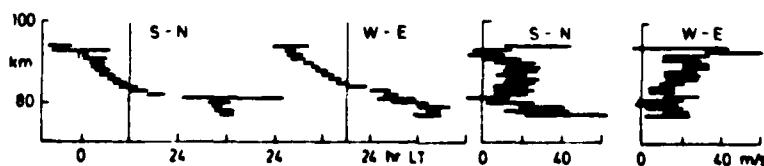


Fig.12. Diurnal wind components at Arenosillo, 24-28 February 1970.

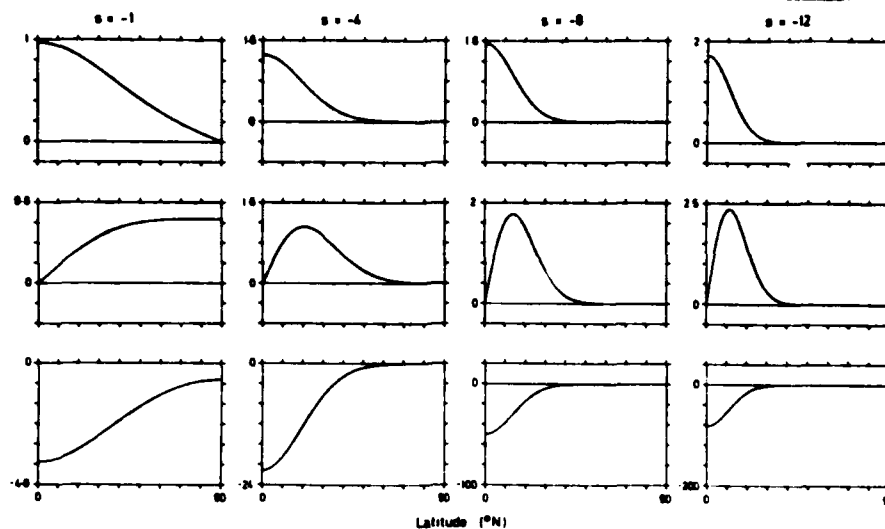


Fig.13. Hough functions Θ (upper row), S-N wind functions Θ_V (middle row) and W-E wind functions Θ_U (lower row) for modes $(1, s, K)$, $s = -1, -4, -8$, and -12 .

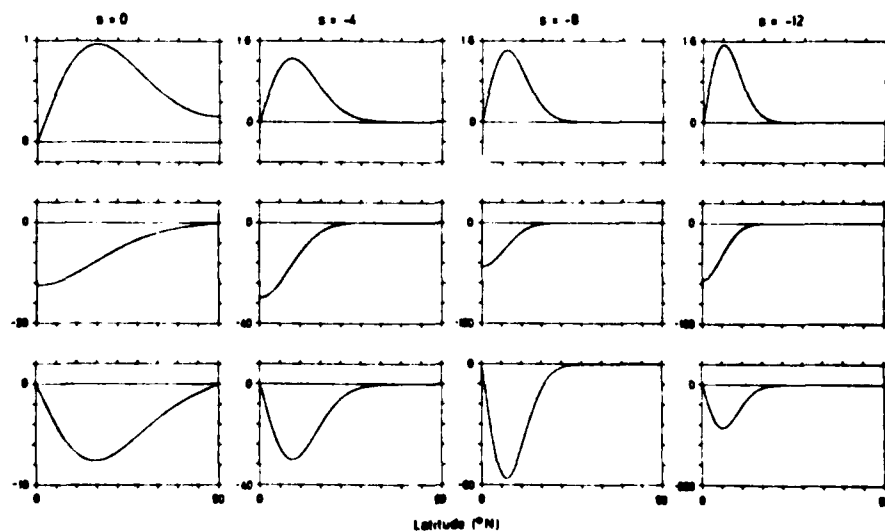


Fig.14. Hough functions Θ (upper row), S-N wind functions Θ_V (middle row) and W-E wind functions Θ_U (lower row) for modes $(1, s, 0)$, $s = 0, -4, -8$ and -12 .

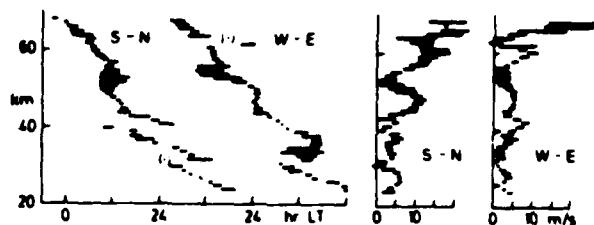


Fig.15. Diurnal wind components at Antigua, 19-20 March 1974.

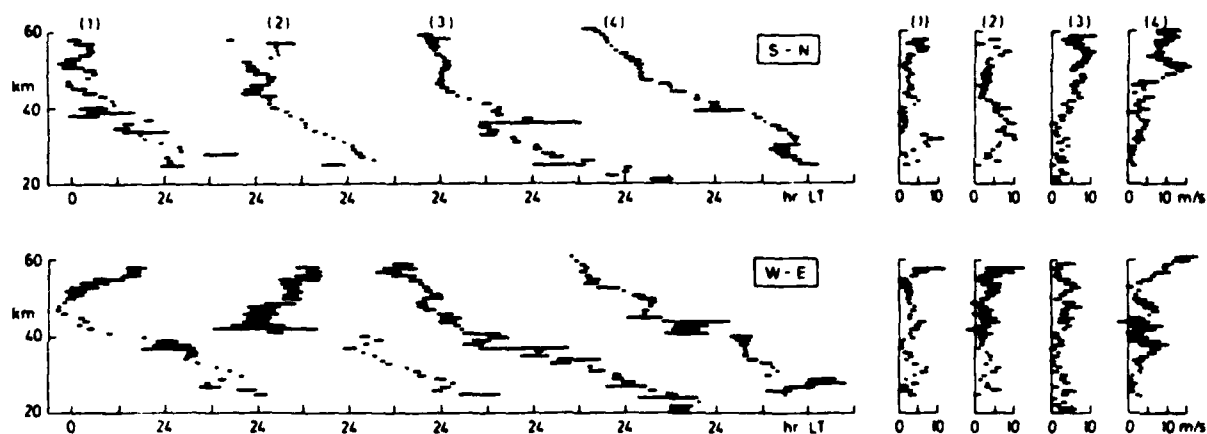


Fig.16. Diurnal wind components at Ascension Island. (1) 11-12 April 1966; (2) 12-13 April 1966; (3) 24-26 October 1968; (4) 19-20 March 1974.

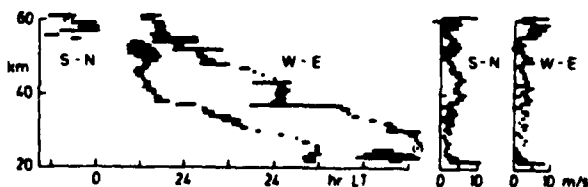


Fig.17. Diurnal wind components at Fort Sherman, 19-20 March 1974.

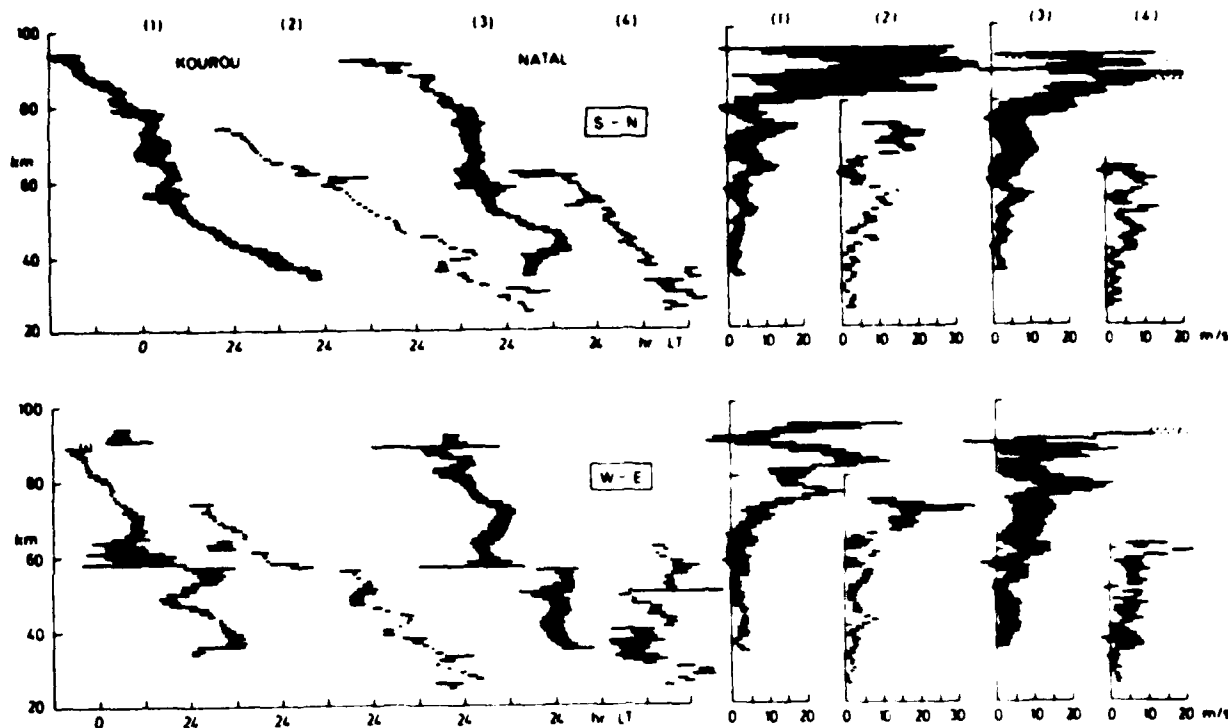


Fig.18. Diurnal wind components at Kourou and Natal. (1) Kourou, 19-20 September 1971; (2) Kourou, 19-20 March 1974; (3) Natal, 1966-68; (4) Natal, 19-20 March 1974.

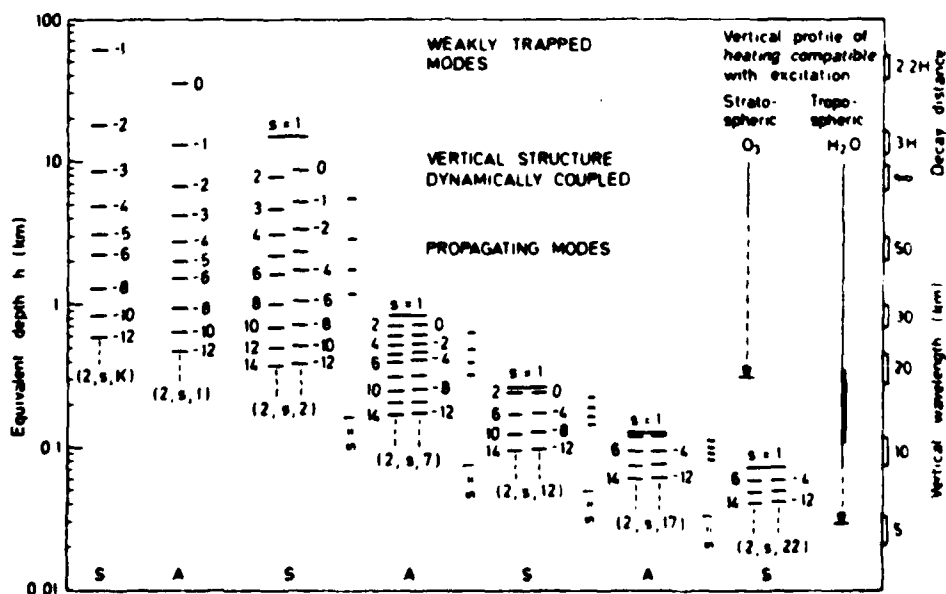


Fig.19. Equivalent depths h of solar semidiurnal Hough modes $(2,s,n)$ for various s and n . (See caption to Fig.2). The short horizontal lines give h for $s = 1$ and the intermediate values of n .

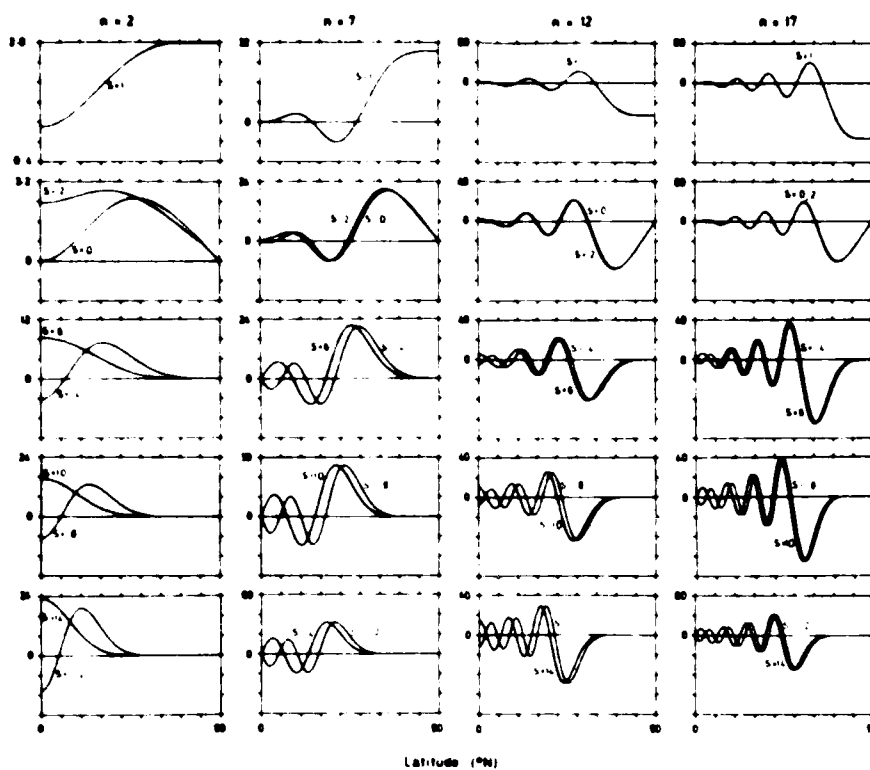


Fig. 20. w-E wind functions Θ_U for modes $(2, s, n)$, $n = 2, 7, 12$ and 17 .

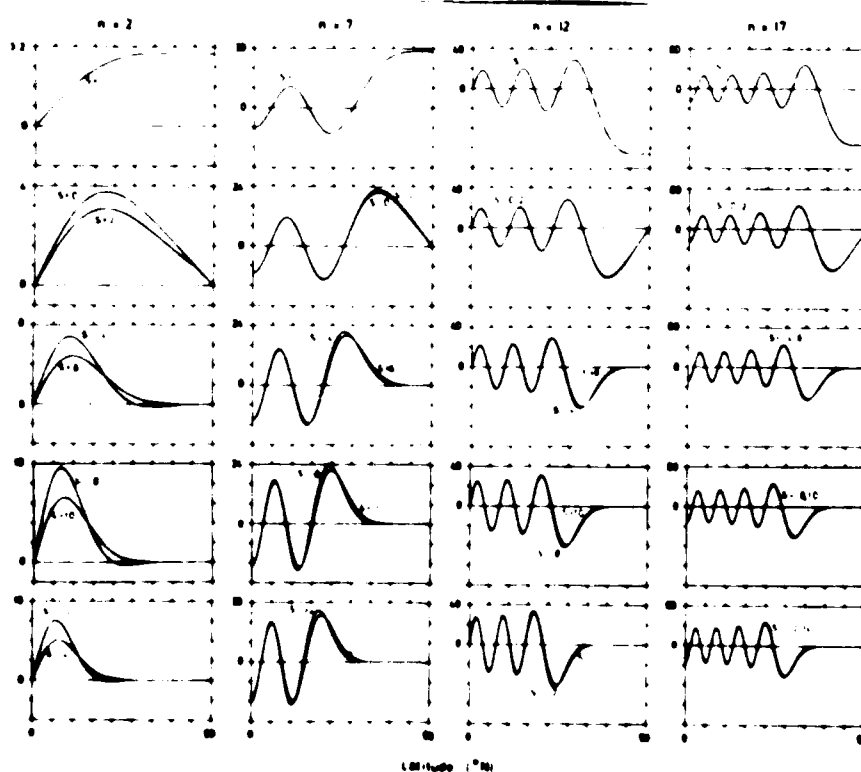


Fig. 21. v-N wind functions Θ_V for modes $(2, s, n)$, $n = 2, 7, 12$ and 17 .

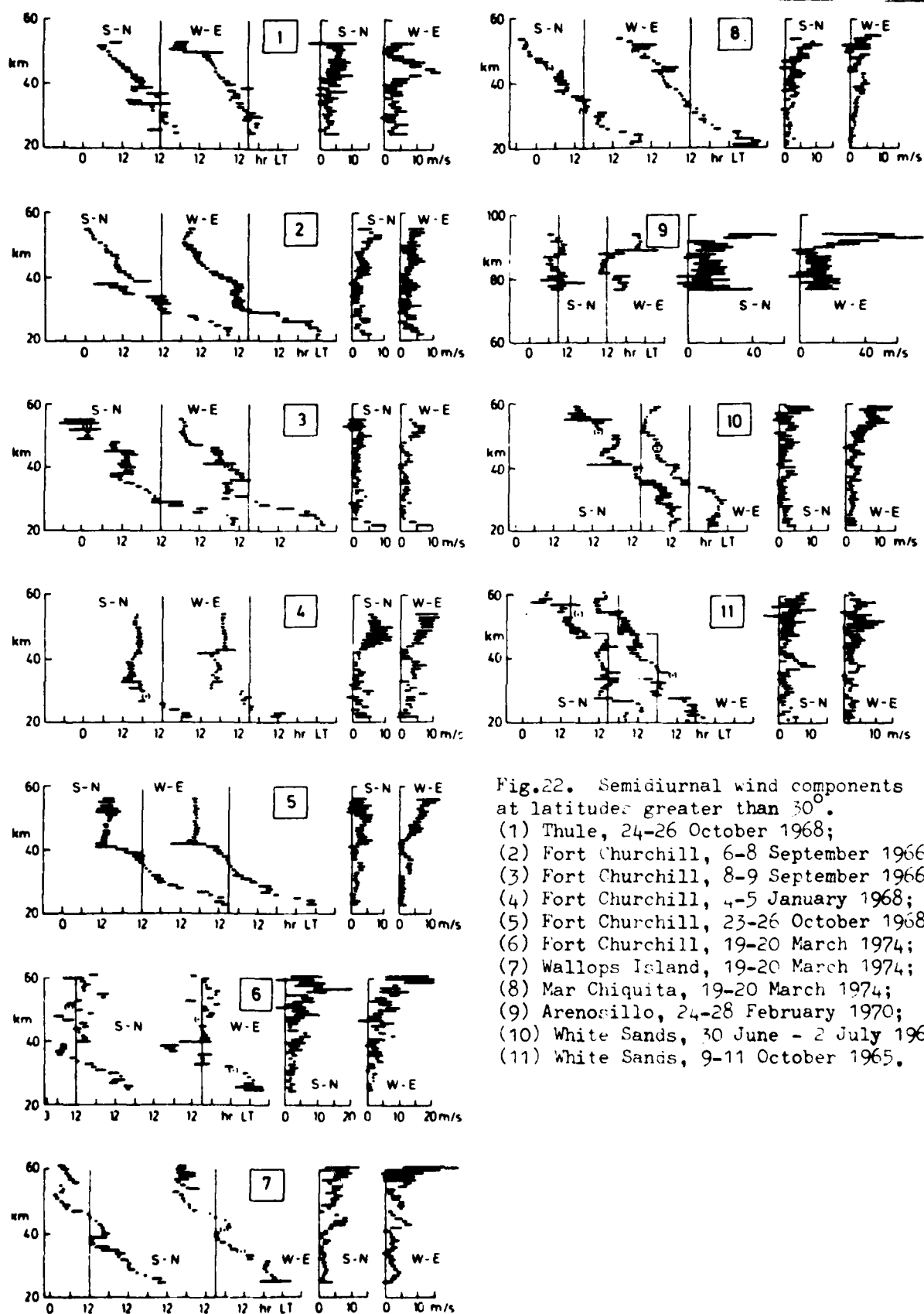


Fig.22. Semidiurnal wind components at latitudes greater than 30° .
 (1) Thule, 24-26 October 1968;
 (2) Fort Churchill, 6-8 September 1966;
 (3) Fort Churchill, 8-9 September 1966;
 (4) Fort Churchill, 4-5 January 1968;
 (5) Fort Churchill, 23-26 October 1968;
 (6) Fort Churchill, 19-20 March 1974;
 (7) Wallops Island, 19-20 March 1974;
 (8) Mar Chiquita, 19-20 March 1974;
 (9) Arenosillo, 24-28 February 1970;
 (10) White Sands, 30 June - 2 July 1965;
 (11) White Sands, 9-11 October 1965.

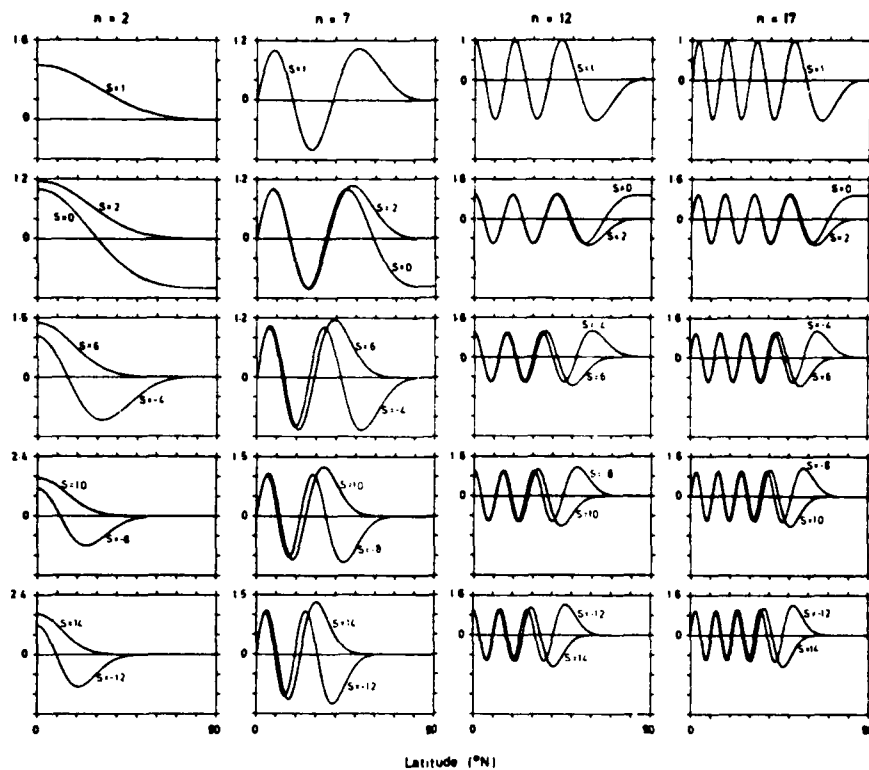
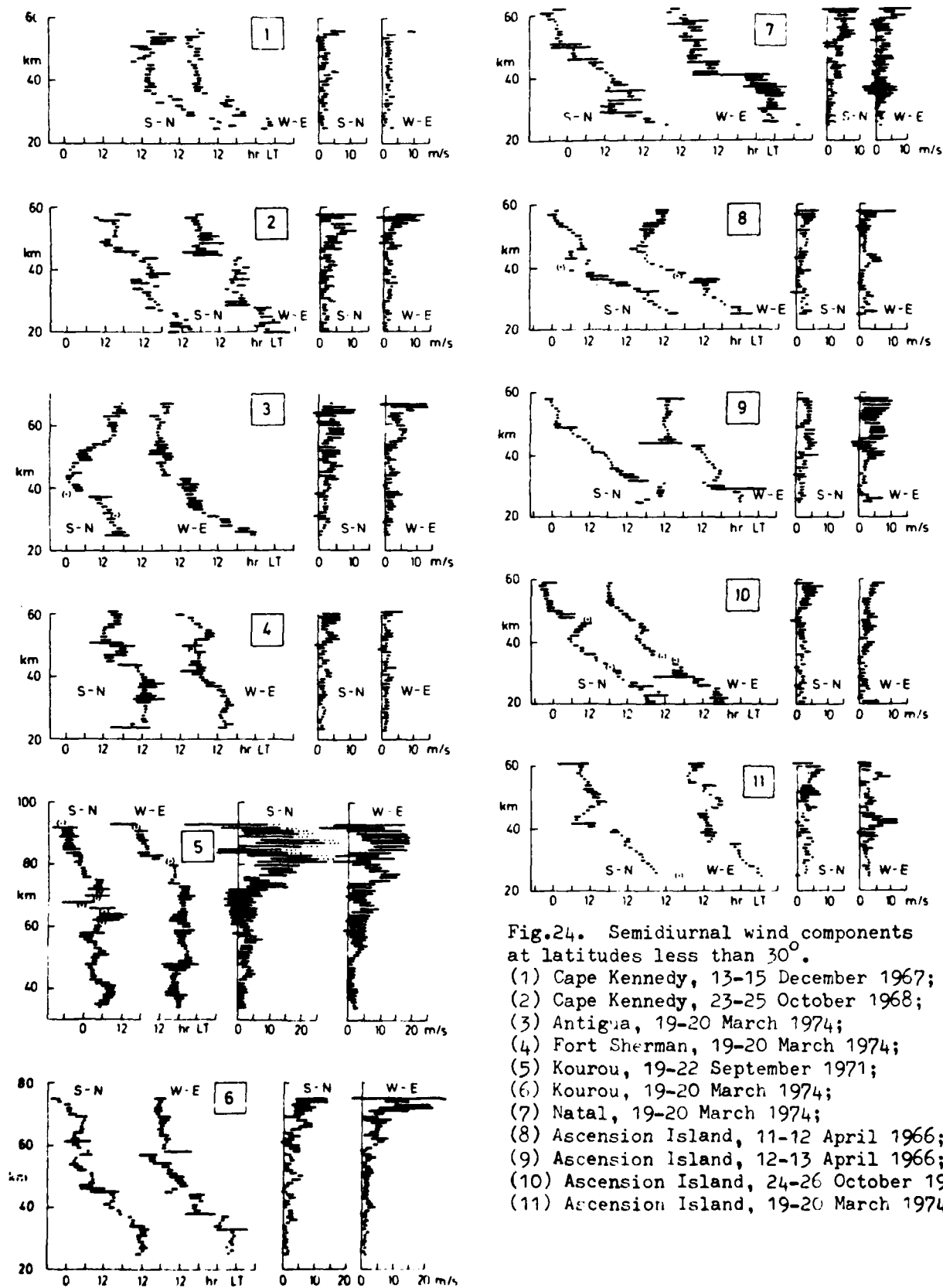


Fig.23. Hough functions Θ for modes $(2, s, n)$, $n = 2, 7, 12$ and 17 .



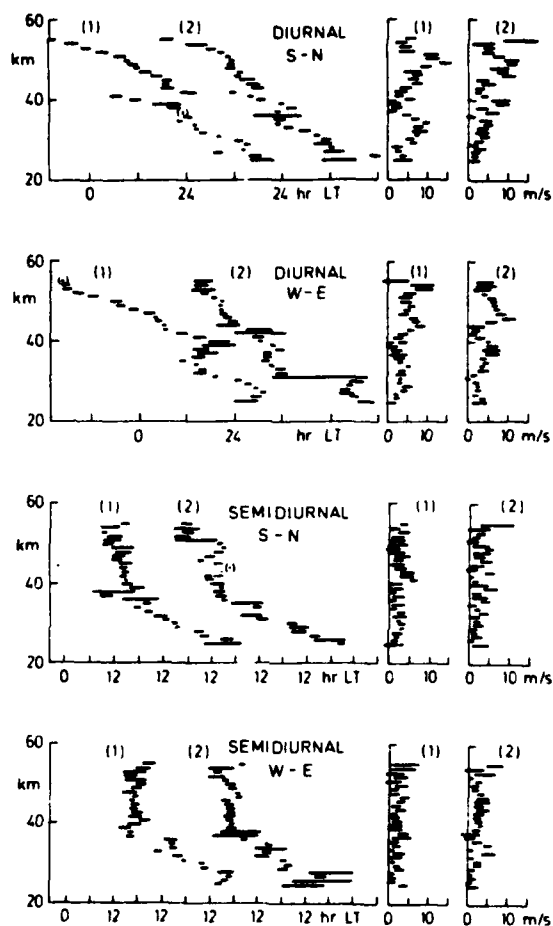


Fig.25. Diurnal and semidiurnal wind components on two consecutive days at Cape Kennedy. (1) 13-14 December 1967; (2) 14-15 December 1967.

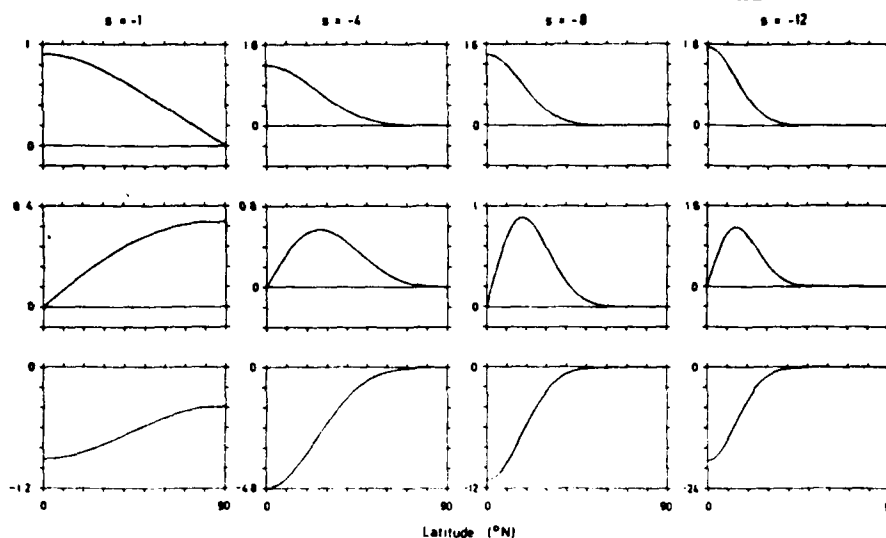


Fig.26. Hough functions Θ (upper row), S-N wind functions Θ_V (middle row) and W-E wind functions Θ_U (lower row) for modes $(2,s,K)$, $s = -1, -4, -8$ and -12 .

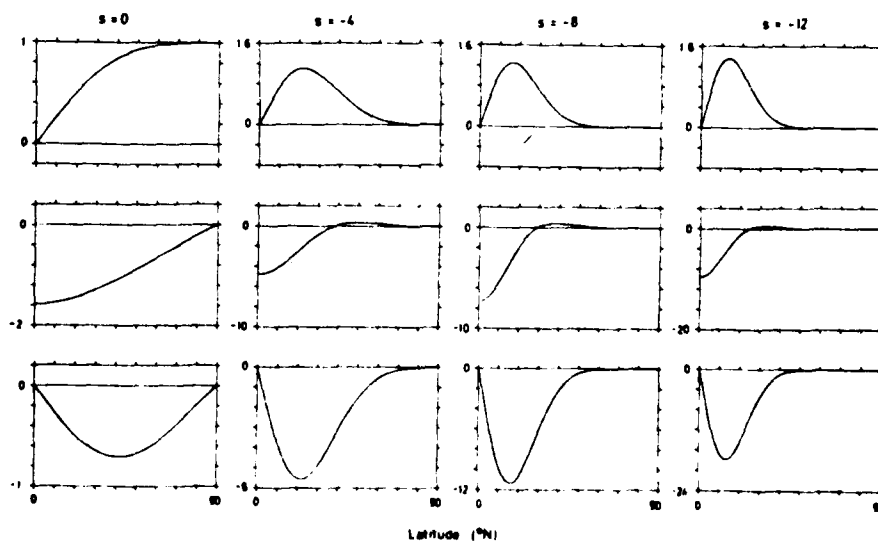


Fig.27. Hough functions Θ (upper row), S-N wind functions Θ_V (middle row) and W-E wind functions Θ_U (lower row) for modes $(2,s,1)$, $s = -1, -4, -8$ and -12 .